


Repetitive transcranial magnetic stimulation recovers cortical map plasticity induced by sensory deprivation due to deafferentation

Ellen Kloosterboer and Klaus Funke 

Department of Neurophysiology, Medical Faculty, Ruhr-University Bochum, Bochum, Germany

Edited by: Janet Taylor & Diego Contreras

Key points

- Partial sensory deprivation (deafferentation) by removing whiskers from the rat snout resulted in a reduced responsiveness of related cortical representations.
- Repetitive transcranial magnetic stimulation (three blocks of intermittent theta-burst) applied for 5 days in combination with sensory exploration restored the normal responsiveness level of the deafferented barrel cortex.
- However, intracortical inhibition (lateral and recurrent) appeared to be reduced after repetitive transcranial magnetic stimulation, probably as the cause of improved responsiveness.
- Repetitive transcranial magnetic stimulation also reduced the asymmetry of the lateral spread of sensory activity.

Abstract Repetitive transcranial magnetic stimulation (rTMS) modulates human cortical excitability. It has the potential to support recovery to normal cortical function when the excitation–inhibition balance is altered (e.g. after a stroke or loss of sensory input). We tested cortical map plasticity on the basis of sensory responses (local field potentials, LFPs) and expression of neuronal activity marker proteins within the barrel cortex of rats receiving either active or sham rTMS after selective unilateral deafferentation by whiskers plucking. Rats received daily rTMS [intermittent theta-burst (iTBS), active or sham] for 5 days before exploring an enriched environment. Our previous studies indicated a disinhibitory effect of iTBS on cortical activity. Therefore, we also expected disinhibitory effects if deafferentation causes depression of sensory responses. Deafferentation resulted in an acute general reduction of sensory responsiveness and enhanced expression of inhibitory activity markers (GAD67, parvalbumin) in the deafferented hemisphere. Active but not sham-iTBS-rTMS normalized these measures. The stronger caudal-to-frontal horizontal spread of activity across barrels was reduced after deafferentation but not restored after active iTBS, despite generally increased responses. Fitting the

Ellen Kloosterboer studied Biochemistry at the Ruhr-University Bochum, where she completed with a Master's degree in 2011. In 2012, she joined the research team 'Experimental Cortical Plasticity' of Klaus Funke (Department of Neurophysiology, Medical Faculty, RUB), where she investigated the influence of transcranial magnetic stimulation on cortical plasticity in the rat and received her doctorate in 2016. **Klaus Funke** studied Biology at the Ruhr-University in Bochum, receiving a diploma (1983) and completing doctoral thesis work (1988) on the central somatosensory system of pigeons. As a postdoctoral student, he joined the group of Ulf Eysel (Department of Neurophysiology, Medical School, Ruhr-University Bochum) studying the state-dependent modulation of retinogeniculate signal transmission (habilitation in physiology 1996). Subsequently, he has built up a research team working on animal models of cortical plasticity and, currently, on the cellular mechanisms of transcranial magnetic stimulation.



LFP data with a computational model of different strengths and types of excitatory and inhibitory connections further revealed an iTBS-induced reduction of lateral and recurrent inhibition as the most probable scenario. Whether the disinhibitory effect of iTBS for the restoration of normal cortical function in the acute phase of depression after deafferentation is also beneficial in humans remains to be demonstrated. As recently discussed, disinhibition appears to be required to open a window for neuronal plasticity.

(Received 28 November 2018; accepted after revision 17 May 2019; first published online 30 May 2019)

Corresponding author K. Funke: Department of Neurophysiology, Medical Faculty, Ruhr-University Bochum, Universitaetsstrasse 150, 44801 Bochum, Germany. E-mail: klaus.funke@rub.de

Introduction

Subsequent to the pioneering studies of Hubel & Wiesel (1964) and Merzenich (Merzenich *et al.* 1983), it is well known that sensory cortical maps show structural reorganization in response to changes in sensory input, in particular with a partial loss of input (deafferentation, deprivation) or more frequent activation of distinct channels with training. In addition to the primary visual cortex, the rodent barrel cortex representing the whisker pad as part of the primary somatosensory cortex has become a model system for cortical sensory map (re-)organization (Feldman & Brecht, 2005; Petersen 2007). The whisker-barrel cortex system is part of the lemniscal trigeminal system, with tactile information being relayed to the primary sensory cortex via the principal nucleus of the fifth cranial nerve and the contralateral medial part of the ventrobasal thalamus. The topographic organization of the whisker pad is mirrored by the cortical barrel field with each barrel (cortical column) representing one whisker (Petersen 2007). Activity-dependent map organization is not only a matter of early cortical development (critical period) (Fox, 1992; Hensch, 2005), but also appears to affect sensory cortical maps in adulthood (Fox, 2002; Feldman & Brecht, 2005). Complete unilateral removal of all whiskers via plucking (Kossut & Hand, 1984) or clipping (Fox, 2008) except for one whisker caused an expansion of the cortical area activated by stimulation of the spared whisker. At the same time, the responses within the deafferented barrels decline (Glazewski & Fox, 1996), apparently as a result of reduced signal transmission to the corresponding barrel (Allen *et al.* 2003; Shepherd *et al.* 2003). Studies at the single cell level indicate that a compensatory redistribution of activity takes place via reallocation of synaptic strengths at individual neurons (Margolis *et al.* 2014). Cortical inputs from spared to deafferented regions showed a higher synaptic strength compared to baseline control, whereas connections between deafferented regions were weakened (Finnerty *et al.* 1999). Recent findings indicate that the distinct spatiotemporal modulation of inhibitory circuits governs the diverse plasticity processes (Froemke, 2015; Letzkus *et al.* 2015). In particular, the fast-spiking class

of interneurons, characterized by the expression of the calcium-binding protein parvalbumin (PV) (Kawaguchi & Kubota, 1998; Markram *et al.* 2004), appears to be involved in preserving a physiological balance of excitation and inhibition at the same time as controlling synaptic plasticity (House *et al.* 2011). This interneuron class constitutes ~40–50% of the inhibitory cortical neurons and, according to its perisomatic type of inhibition, appears to be most important for controlling the output activity of pyramidal cells and thereby cortical excitability in general. These interneurons control the temporal pattern of network activity and, in particular, the occurrence of synchronous oscillations within the gamma range (Cardin, 2018). Furthermore, these neurons appear to quickly adapt to the current physiological state of the neuronal network, in particular during different phases of learning and memory consolidation, by changing PV expression and the ratio of excitatory to inhibitory input (Caroni, 2015). Changes in the expression of the calcium-buffering PV affect synaptic GABA release (Caillard *et al.* 2000), the occurrence of gamma-oscillations (Vreugdenhil *et al.* 2003) and the characteristics of the fast-spiking patterns (Orduz *et al.* 2013). Malfunction of these neurons appears to be a major cause of the cognitive deficits being a part of neuropsychiatric phenotypes such as schizophrenia (Benes & Berretta, 2001; Lewis, 2014; Volk & Lewis, 2014; Gonzalez-Burgos *et al.* 2015). It is conceivable that they also contribute to cortical map reorganization during disturbed sensory input or central processing, such as may occur after a trauma or stroke.

Manipulation of cortical inhibition in general, or of the activity of a distinct subsystem such as the PV+ interneurons, could be beneficial for treating acute or chronic neurological symptoms if these are related to a miss-balance of inhibitory-to-excitatory activity. Because systemic pharmacological approaches are often confounded by severe side-effects and loss of effects as a result of adaptation, the neuromodulatory actions of non-invasive brain stimulation techniques appear to be promising (Di Pino *et al.* 2014). Repetitive transcranial magnetic stimulation (rTMS) has been shown to either raise or dampen cortical excitability depending on

the type of stimulation protocol (Ziemann und Siebner, 2008; Ridging & Ziemann, 2010; Dayan *et al.* 2013). In the case of stimulating the somatosensory cortex with an excitatory protocol of 5 Hz or intermittent theta-burst stimulation (iTBS) pattern, an increase in cortical excitability was found associated with improved tactile perception (Tegenthoff *et al.* 2003; Ragert *et al.* 2008). Originally, these effects had been attributed to the induction of long-term potentiation and depression (LTP, LTD) (Thickbroom, 2007). However, the after-effects measured with motor-evoked potentials in humans are usually transient, disappearing after 30–60 min. In our previous studies on rat rTMS models, we found evidence for the modulation of inhibitory cortical systems. Rats treated with iTBS showed a dose-dependent (number of blocks) reduction in the number of interneurons with a high-level of PV expression (>50% of range) (Benali *et al.* 2011; Funke & Benali, 2011; Volz *et al.* 2013). As verified by co-labelling with markers of the perineuronal nets of these interneurons, the neurons did not die but, instead, strongly reduced their PV expression within 30–40 min (Benali *et al.* 2011; Hoppenrath & Funke, 2013). This was accompanied by increased tactile responses in rat barrel cortex (Thimm & Funke, 2015), improved tactile learning in rats during the after-effect period (Mix *et al.* 2010) and restored early visual cortex development in the absence of visual input during the critical period (Castillo-Padilla & Funke, 2016). The reduction in the number of 'high-PV' interneurons following iTBS could last for a couple of days without further interventions (Benali *et al.* 2011) but recovered to control levels if rats performed a learning task (Mix *et al.* 2010). This fits well with the theory proposing that a transient disinhibition opens a window for synaptic plasticity processes (Letzkus *et al.* 2015; Vlachos *et al.* 2012). A good example is the dynamic regulation of parvalbumin expression in hippocampal interneurons according to recent experience (Caroni, 2015): fear conditioning increased the number of 'high-PV' neurons, whereas exploration of an enriched environment decreased them. The former group showed a decreased ability to learn afterwards, whereas the latter showed improved learning, which is obviously a mechanism preventing 'unwanted' but promoting advantageous memories. Furthermore, 'high-PV' neurons exhibited an increased number of glutamatergic inputs, whereas this was decreased for 'low-PV' neurons. We found a similar relationship for neocortical neurons and could also show that the switch from high- to low-PV neurons after iTBS is accompanied by reduced activity of glutamatergic inputs to these neurons (Jazmati *et al.* 2018).

Deprivation of sensory input has been shown to not only reduce the spatial extent of cortical representations in rodents (see above), but also reduce cortical excitability and the size of representations in humans after limb

immobilization (Facchini *et al.* 2002; Lissek *et al.* 2009; Ngomo *et al.* 2012). These effects were already evident after few days, and thus during an acute phase of imbalance of cortical sensory activation. Lissek *et al.* (2009) reported that tactile acuity correlated with cortical activation as measured by functional resonance imaging was reduced on the immobilized side, whereas it was increased on the contralateral side. We therefore expected that the potential disinhibitory action of iTBS-rTMS may counteract the depressive effects of immobilization or deafferentation as used in our studies. To test this assumption, we used the well-established barrel cortex model with partial cortical deafferentation by whisker plucking (Diamond *et al.* 1993) in combination with iTBS-rTMS. Changes in the spatial distribution of sensory evoked activity were analysed with electrophysiological recordings from four neighbouring barrels, including two central non-deafferented barrels flanked by deafferented barrels, using an electrode array (Fig. 1, LFP-recordings), as well as by immunohistochemical analysis of neuronal activity markers in flattened horizontal sections through the barrel cortex. We compared three groups: two groups with unilateral barrel field deafferentation (all whiskers on the left side plucked except for the arcs no. 2 & 3), with one group receiving active iTBS and the other receiving sham iTBS, in addition to a control group without barrel field deafferentation. On a daily basis, all rats experienced a new enriched environment to guarantee that the remaining whiskers had been stimulated. This appears to be a requisite because neuronal plasticity is usually driven by activity, which is also a matter for consideration in human training programs. Control of how sparse or intense whisker use is cannot be achieved when rats are housed in a standard cage.

In the case of evoked local field potential (LFP) recordings, we selectively stimulated individual whiskers of the spared arcs and measured the lateral spread of activity across neighbouring cortical barrel regions. In the case of the immunohistochemical studies, we achieved the selective stimulation of only one whisker arc by clipping all of the whiskers on the experimental side except for arc no. 2 (controls and deafferented rats) before the rats experienced the enriched environment one final time before being killed. In this way, we were able to perform multiple comparisons of neuronal activity/plasticity marker expression between stimulated and non-stimulated arcs, previously deafferented and non-deafferented arcs, and the normal state of the contralateral hemisphere (internal control). Deafferented rats receiving sham-iTBS not only showed reduced evoked responses amplitudes in the spared barrels, but also reduced lateral spread of activity to neighbouring barrels, whereas active iTBS-treated rats showed normal response amplitudes but a stronger lateral spread of activity compared to controls (primarily in a rostral direction).

The latter appeared to be related to a reduced cortical inhibition because the response suppression elicited via a whisker double stimulation paradigm was strongly diminished following active iTBS but was not affected by deafferentation. A simple computational model, implementing feed-forward, recurrent and asymmetric lateral inhibition between barrels, was able to mimic the experimental findings and thus supports the hypothesis of a disinhibiting action of iTBS-rTMS.

Methods

Ethical approval

All experimental procedures had been approved by the ethics section of the local government (LANUV, Az.

87-51.04.2010.A097) and are in compliance with the guidelines of the animal welfare laws in Germany and the European Union. The investigators noted, understood and followed the ethical principles under which the journal operates and confirm that their work methods comply with the UK regulations (Grundy, 2015).

Experimental groups

Male Sprague–Dawley rats aged 3–4 months old (weighing 420–510 g; Janvier Labs, Le Genest-Saint-Isle, France), housed in groups of three or four in standard macrolon cages with free access to food pellet and water, were randomly divided into three groups by a technician: in two groups, all whiskers of the left pad except for arcs

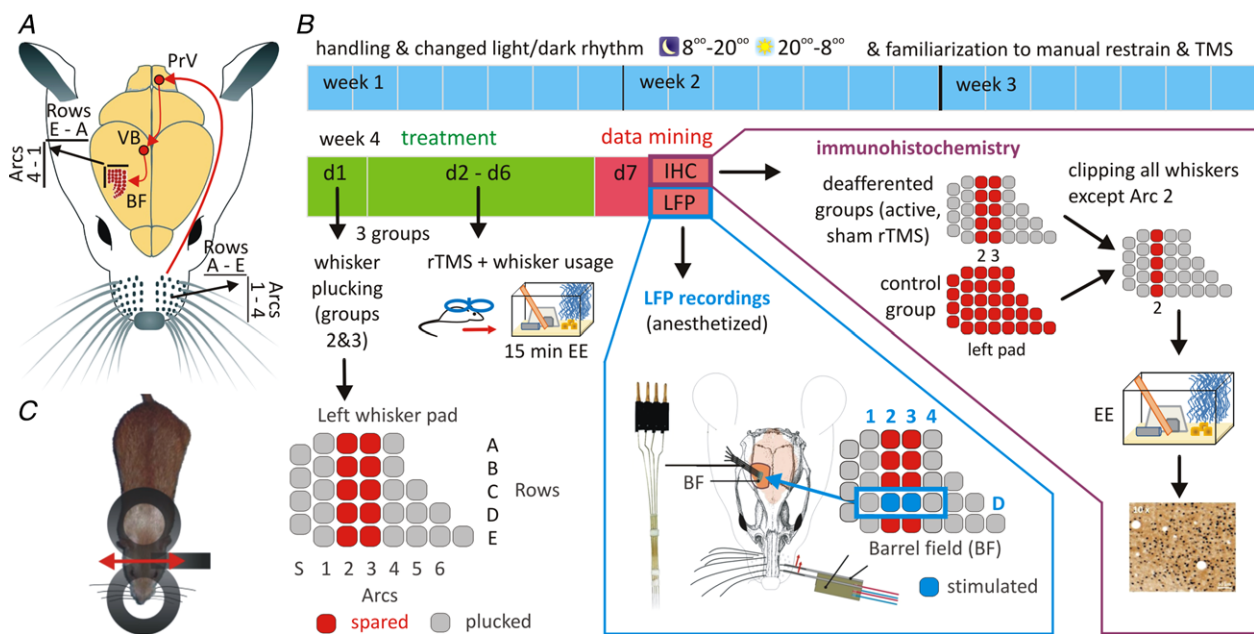


Figure 1. Experimental design

A, the whisker–barrel cortex system is part of the trigeminal lemniscal somatosensory pathway built by the primary afferents within the trigeminal nerve, the thalamically projecting neurons of the principal nucleus of the fifth cranial nerve (PrV), the cortically projecting neurons of the ventrobasal thalamic nucleus (VB) and the cortical barrel field (BF). The topography of the pad of whiskers at the snout is mirrored by a corresponding arrangement of cortical columns (barrels) organized in rows A–E and a number of arcs (1–4 indicated, the more caudally located 4 ‘stradlers’ α to δ are omitted for clarity because they do not belong to the row and arc system). B, experimental design: after 3 weeks of habituation to an altered light/dark rhythm, familiarization to handling and manual restraint by the experimenter and the sound and sensations of TMS, rats were divided into three groups: one group (no. 1) without removal of any whisker (controls) and two groups (no. 2 & 3) with unilateral deafferentation by plucking all whiskers of the left pad except those of arcs 2 & 3 on day 1 (d1) of the fourth week, followed by 5 days of either active (one group) or sham (other group) rTMS (d2–d6). C, showing how the figure-of-8 coil was centred above the rat’s head to induce a mediolaterally oriented electric field within the brain. All groups explored an EE on a daily basis (d2–d6) to force whisker use. At d7, the groups were split into two halves, with one-half investigated by LFP recordings across spared and neighbouring deafferented barrels (D1–D4, blue frame) and the other analysed for changed activity/plasticity marker expression by immunohistochemistry (purple frame). To achieve an identical and selective stimulation of only one whisker arc in all animals prior to marker analysis, all whiskers of the left pad except those of arc no. 2 were clipped for the control group, whereas, for the previously deafferented animals, arc no. 3 was clipped. The whisker pad of the right side was not manipulated to serve as an internal control. Afterwards, rats explored a new EE again to enable use and stimulation of the remaining whiskers.

no. 2 & 3 were removed by plucking. One group received iTBS for 5 days (termed 'active', details below), whereas the other group received sham-iTBS ('sham') treatment. This protocol of repetitive TMS was chosen because it usually enhances cortical excitability in humans (Huang *et al.* 2005) and rats (Thimm *et al.* 2015), most probably because of a disinhibitory effect (Schmidt-Wilcke *et al.* 2018). Animals were allowed to explore a daily changing (enriched) environment (EE) (3×15 min) to force the active use of the whiskers. Otherwise, when in a standard cage without objects to explore, rats may be in a sensory deprived state that is not comparable to a human situation, in particular with concomitant sensorimotor rehabilitation training. A third group served as controls, not being deafferented and not being subjected to sham or active iTBS but, instead, to exploration of the same enriched environments to achieve a similar state of sensory experience and whisker use as that in the experimental groups. Of these groups, around one-half of the animals were investigated electrophysiologically ($10 \times$ active iTBS, $10 \times$ sham iTBS, $4 \times$ controls), whereas the remainder were analysed by immunohistochemical means ($6 \times$ active iTBS, $6 \times$ sham iTBS, $5 \times$ controls). In total, 42 rats had been used but one rat of the LPF control group had to be excluded as a result of noisy records (group size reduced from five to four). The numbers of animal were kept as small as possible according to the 3Rs rule (Replacement, Reduction and Refinement), in addition to considering statistical requirements. The group of untreated control animals was smaller because we expected less variability.

Targeted whisker stimulation during the electrophysiological recordings (LFPs from D1–D4) was achieved with the aid of piezoelectric bending actuators (either whisker D2 or D3; see below). We selected the row of barrels D1–D4 for the recordings because it crosses arcs 1 to 4, with arcs 1 and 4 deafferented and sparing arcs no. 2 & 3 in the middle. By applying the same stimulation protocol to deafferented and control animals, we compared not only the response amplitude of the non-deafferented barrels (either arc 2 or 3), but also the lateral spread of activity to the neighbouring barrels, which were either deafferented or not. To achieve a similar situation in the case of the immunohistochemical analysis of neuronal activity and plasticity markers, we aimed to stimulate only one arc prior to analysis. Therefore, we clipped all whiskers of the left (experimental) side, except for arc no. 2, both for the control rats and the two previously deafferented groups (here arc no. 3 was removed). The right whisker pad remained unchanged to serve as an internal control for all groups. Then, rats explored the enriched environment for a final time for 30 min to enable active use and stimulation of the remaining whiskers before being killed (Fig. 1B).

Familiarization of rats with the experimental procedures

The experimental part of the study was preceded by 3 weeks during which the animals were first adapted to a changed dark-light rhythm (lights on from 20.00 h to 08.00 h). Already at that time, the rats were familiarized with the experimenter as a result of daily handling (2 h day^{-1} , moving between cages, playing with objects). Thereafter, rats were adapted to the room and table where the TMS took place. In a stepwise procedure, rats were familiarized with the sound generated by the TMS and the skin sensations evoked by single pulses or single bursts (3 at 50 Hz). Simultaneously, the rats were adapted to manual restraint lasting for at least the duration of an iTBS stimulation block (600 pulses, 190 s). Rewards were given if the rats tolerated this procedure without moving too much. Rats were restrained by fixating the body and head with both hands and with the index fingers flanking the head. With the coil fixed above the rat's head, guiding the head was performed to achieve a proper brain-to-coil distance. Rats were further adapted to the box that later housed the enriched environment. All experimental procedures were performed in dimmed light in accordance with the animal's 'low-light daytime'. Animals were housed in standard cages in groups of three (if not in the enriched environment) with free access to food pellets and tap water.

Whisker plucking/clipping

One day before starting the iTBS sessions, rats were sedated using Medetomidin hydrochloride [0.05 mg kg^{-1} body weight (BW) i.p.] (Vetoquinol GmbH, Ravensburg, Germany) and with the left whisker pad anaesthetized with 2% lidocain gel. Using strong forceps, individual whiskers were plucked (including tiny secondary whiskers of the same follicle), sparing arcs no. 2 & 3. Control animals underwent the same procedure, although only applying force to the whiskers without plucking them. Recovery of the animals from sedation was forced by applying Atipamezol hydrochloride (1.6 mg kg^{-1} BW i.p.) (Vetoquinol GmbH) when rats were placed on a heat pad and they were supervised until motor activity recovered completely. During the course of the 5 days with rTMS and EE, the manipulated whisker pad was checked daily for newly grown whiskers at the previously plucked follicles and cut with a scissors if present. Those animals used for the immunohistochemical part of the study were also briefly sedated and all whiskers except for arc no. 2 of the left pad (deafferentation side) were clipped with a scissors before the animals experienced a new enriched environment for a final time.

At the beginning of the experiments, whiskers were plucked because they grow quickly ($\sim 1 \text{ mm per day}$),

so that initially short and then growing whiskers could be used for tactile exploration. In between and prior to final EE exposure, in the case of histological analysis, it was sufficient to clip the whiskers because the relevant time intervals were short.

iTBS-rTMS

Repetitive transcranial magnetic stimulation using the iTBS protocol was applied to conscious rats after familiarization with the procedure as described above. The rats received no sedation and had learned previously to keep the head in a position guided by the index fingers of the experimenter. On five subsequent days, rats received 1800 pulses per day, split into three blocks of 600 pulses applied at intervals of 15 min. The same type of stimulation had been found to improve tactile learning (Mix *et al.* 2010) and to be superior to a single block for reducing the number of PV+ cells (Volz *et al.* 2013) and increasing somatosensory responses (Thimm & Funke, 2015). Each block resembled a typical iTBS pattern with 20 TBS trains repeated every 10 s (Huang *et al.* 2005). Each train was composed of 10 bursts (three pulses at 20 ms intervals) applied at a periodicity of 5 Hz. A conventional figure-of-eight coil (2×70 mm; MagStim, Whitland, UK) was fixed by a stand and the head of the rat was centred below the coil at a coil-to-head orientation inducing a mediolaterally orientated electric field. The stimulator (MagStim rapid2) output was set to 23% of maximal machine output power and the distance between the coil and head was varied between 5 and 10 mm to identify a position just subthreshold for evoking muscle twitches by applying single TBS bursts when guiding the rat's head with the index fingers. Then, during iTBS, this position was kept but slightly varied if muscle twitches occurred (checked visually and by sensing with the hands). With this procedure, almost identical stimulation conditions could be achieved, with the stimulation intensity being $\sim 90\%$ of motor threshold. Although we could not explicitly measure motor threshold, we did not find a change in threshold over time as would be evident by a changed distance between the coil and head when testing threshold intensity.

Given these settings, a mediolateral orientation of the induced electric field should be suitable to evoke spiking activity primarily within the axons of the corpus callosum but not directly within the cortical areas or within sub-cortical structures. Using a sphere model of rodent head, Tang *et al.* (2016) calculated the strength of an electric field induced by a conventional figure-of-eight coil to be ~ 150 V m⁻¹ at a distance of 10 mm from coil surface with maximum machine output, corresponding to ~ 130 V m⁻¹ at the depth of the corpus callosum (Tang *et al.* 2016). Thus, ~ 30 V m⁻¹ would be induced with 23% machine output, or 30 mV mm⁻¹ when scaled down

to the dimensions of the callosal axons. This appears to be sufficiently strong to depolarize these axons along the horizontal path of ~ 10 mm across the brain midline before bending downwards (maximum 300 mV difference). In the case of sham stimulation, the distance between the coil and the rat's head was increased to 200 mm.

Using the large figure-of-eight coil for stimulation, we could not achieve a focal stimulation of the barrel field. As in our previous studies, we aimed to stimulate the callosal fibres and thereby manipulated cortical activity primarily within layers 2–4. A recent study showed that this type of stimulation primarily targets inhibitory interneurons within the superficial cortical layers but did not activate layer 5 pyramidal cells even with 100% stimulation intensity (Murphy *et al.* 2016).

Enriched environment

To ensure that all rats used their whiskers to a similar degree after iTBS had been applied, single rats were placed in an EE for 15 min. The EE was composed of many different objects (tubes, bottles, cups, spheres, strings hanging from the ceiling) made of different materials (plastic, wood, cardboard, metal). Cardboards and tubes divided the arena in smaller compartments. Occluded food awards [e.g. peanuts, Fruit-Loops (Kellogg's, Battle Creek, MI, USA), banana chips] furthered motivation with respect to exploring the arena. The complexity of the EE was increased from day to day to avoid stress at the beginning and to keep motivation high toward the end. Rats explored the EE in darkness to focus attention on the tactile domain and were video-monitored (infrared) for offline analysis of activity. The latter revealed that all rats were actively exploring the new arena and no obvious differences were evident between rats.

Electrophysiological recordings

Rats were initially anaesthetized with urethane (1.6 g kg⁻¹ BW I.P.; Sigma, St Louis, MO, USA) followed by ketamine hydrochloride (0.06 g kg⁻¹ BW I.P.) (CP-Pharma GmbH, Burgdorf, Germany) to achieve sufficient analgesia during the surgery phase. The body temperature was kept at 37.5°C by the aid of a heat plate (ATC1000; WPI, Friedberg, Germany) continuously regulated via a rectal thermistor in a feedback loop. After complete analgesia had been achieved (checked by corneal reflex and squeezing toes), the scalp was incised by a longitudinal cut, and then the cranium was exposed and trepanned above the right barrel cortex. After careful opening of the dura mater, first a single polyamide insulated tungsten electrode (~ 1 M Ω , 125 μ m) was lowered to layer 4 to determine the positions of barrels D1 to D4 when repeatedly stimulating the corresponding whisker (principal whisker) with a piezoelectric bending

actuator (P-871.127; Physik Instrumente GmbH and Co KG, Karlsruhe, Germany) at 2 s intervals (1.72° at 600° s^{-1} in the anterior–posterior direction with slower return by 150° s^{-1}). Short latency (8–10 ms) single unit spike responses were taken as an indication of input from the whisker topographically related to the recorded barrel compared to weaker and slower responses when stimulating neighbouring whiskers. Thereafter, an array of four polyamide insulated tungsten electrodes (0.5 M Ω , 125 μm , 300 μm spacing between electrodes) was lowered first to layers 2/3 and later to layer 4 to record local field potentials. Electrode arrays were custom-made to best fit the spacing of barrels in row D of the 4–5-month-old Sprague–Dawley rats as previously determined by histology. At the end of the electrophysiological experiments, rats were killed by perfusion when under deepened anaesthesia (pentobarbital sodium 500 mg kg $^{-1}$ BW; Narcoren; Boehringer Ingelheim Vetmedica GmbH, Ingelheim am Rhein, Germany) to enable histological verification of electrode tracks (see below).

Histochemistry

Rats destined for the immunohistological analysis were deeply anaesthetized (pentobarbital sodium, 500 mg kg $^{-1}$ BW; Narcoren) 30 min after exploring the EE and transcardially perfused first with ice-cold Ringer solution (with 5000 IE of heparin added), followed by cooled 4% paraformaldehyde in PBS. After the brains had been post-fixed for 2 days, the neocortex of both hemispheres including the barrel cortex was carefully dissected from the brain, flattened between two polyamide grids and stored in 30% sucrose (in PBS) for 3 days. Before preparing 20 μm thick horizontal cryosections through layers 2/3 and 4, three vertical holes, building the edges of a rectangle, were punched around barrel cortex to exactly orient and align sections from different layers using NeuroLucida software (MicroBrightField Europe e.K., Magdeburg, Germany). Alternating sections were used for immunohistochemical labelling of c-Fos, zif268 (egr-1), 67 kDa isoform of glutamic acid decarboxylase (GAD67) and PV, as well as cresyl violet and cytochrome oxidase staining. One section per animal was first tested for histological quality via cresyl violet (Nissl) staining.

Immunohistochemical stainings were performed in accordance with earlier studies (Trippe *et al.* 2009; Benali *et al.* 2011). The primary antibodies used for staining neuronal marker proteins were: GAD67 (monoclonal; dilution 1:2000, clone 1G10.2; Millipore, Billerica, MA, USA), PV (monoclonal; dilution 1:1000, clone 234; Swant, Bellinzona, Switzerland), zif268 protein (rabbit anti-Erg-1, polyclonal; dilution 1:1000; Santa Cruz Biotechnology, Sanata Cruz, CA, USA) and c-Fos protein (polyclonal; dilution 1:1000; Santa Cruz Biotechnology).

Visualization of specific labelling was carried out using 3,3'-diaminobenzidine (DAB) as chromogen, intensified by adding ammonium-nickel-sulphate. Barrels within layer 4 were visualized via cytochrome oxidase staining according to Wong-Riley (1979), using cytochrome C (C-2506; Sigma) and DAB for visualization. Therefore, dissected rat brain slices were carefully washed in phosphate buffer (pH 7.4) and subsequently transferred to a solution of 0.6% DAB, 0.3% cytochrome C and 5% sucrose in phosphate buffer. Slices were incubated at 37°C for 2 h, washed in phosphate buffer and afterwards transferred to microscope slides or prepared for DAB-nickel staining as described above.

Histological verification of the recording sites was performed on flattened horizontal sections of the right hemisphere. Electrode tracks were visualized by immunohistochemical detection of extravagated serum protein (biotinylated rabbit-anti-rat antibody; dilution 1:1000, BA4000; Vector Laboratories, Inc., Burlingame, CA, USA).

Data analysis

LFPs of barrels D1–D4 were analysed with regard to the absolute amplitude of the N1 and P1 waves with reference to the mean of a 500 ms baseline episode prior to whisker stimulation (Fig. 2Aa). In the case of double-stimulation of one whisker, the amplitude of the first N1 wave (N1₁) was also determined with reference to prestimulation baseline, whereas the amplitude of the second N1 wave (N1₂) (Fig. 3Aa) was measured between the most positive value between N1₁ and N1₂ and the peak of N1₂. Suppression of the second response was determined by the ratio of the second to the first response (N1₂/N1₁). Determination of LFP amplitudes followed a standardized procedure. Random numbers were assigned to the experimental animals to ensure that the experimenter was blinded with regard to group assignment of the animals. In the case of immunohistological analysis (counting labelled cells), the experimenter was blinded by arbitrary numbers assigned to tissue sections of each animal by a technician.

Labelled cells were counted if the staining intensity of the soma exceeded a fixed threshold settled above the background stain that results from additional staining of the neuropil. In the case of PV, previous studies have shown that changes in somatic labelling intensity induced by experimental procedures such as different behavioural conditioning (Caroni, 2015) or rTMS (Benali *et al.* 2011; Jazmati *et al.* 2018) primarily affected the ratio of cells showing either very high or very low labelling intensity ('high-PV' vs. 'low-PV' cells). Accordingly, we set the threshold at 50% of maximal somatic PV-labelling intensity to count the number of high-PV cells. In a first attempt, labelled cells (c-Fos, zif268, GAD67, PV)

on the experimental side were separately counted for each arc of barrels. Afterwards, arcs were grouped by the different experimental conditions: (i) directly stimulated before by whisker use (only arc 2); (ii) previously spared from deafferentation but not stimulated as a result of

clipping whiskers (only arc 3); and (iii) all deafferented arcs (no. 1, 4–7 and straddlers) with numbers of labelled cells averaged. In the case of the contralateral side (internal control) labelled cells of all barrels were averaged because all were stimulated before. Statistical analysis of

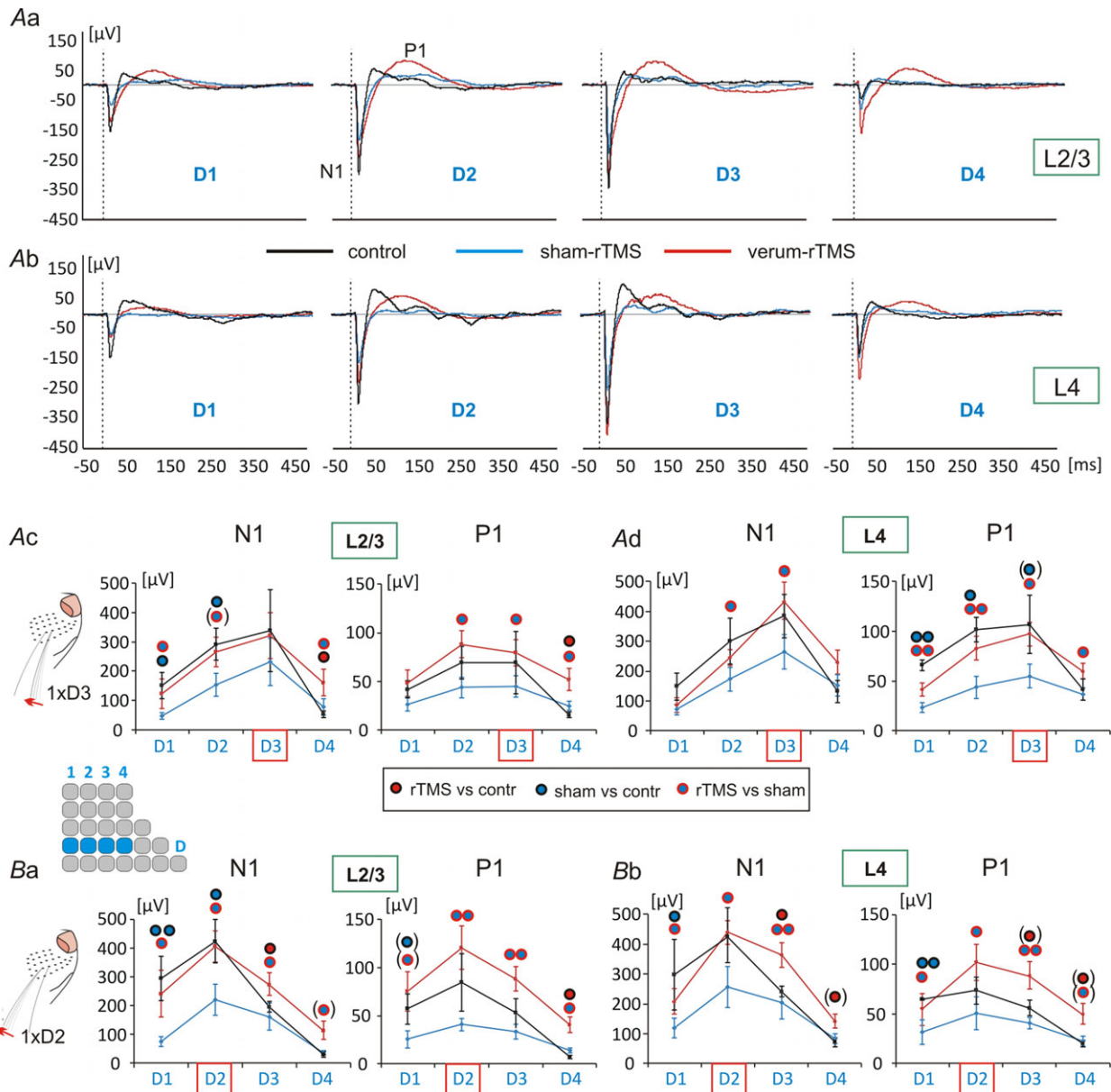


Figure 2. Simultaneous LFP recordings from barrels of row D

Aa and Ab, grand average LFPs (mean of all rats per group) evoked with stimulation of whisker D3 and recorded from the representations of D1–D4 in layer 2/3 (Aa) and layer L4 (Ab) of the three groups: controls (black), deafferented-sham (blue) and deafferented-active rTMS (red). Statistical analysis of the two LFP components N1 and P1 for layers L2/3 (Ac), and L4 (Ad) showing the mean \pm SEM. Ba and Bb, showing the same analysis as in (Ac) and (Ad) but with stimulation of whisker D2. Red frames at the abscissa indicate which whisker had been stimulated (see also barrel field inset). Coloured dots indicate significant differences for pairwise comparison between groups (U test); red circle filled blue: sham vs. active rTMS group. Number of dots indicates significance level: 1: $P < 0.05$; 2: $P < 0.01$. Symbols in brackets indicate P values between 0.05 and 0.1 (strong trend). Number of animal included per data set (outliers excluded): (Ac) D1: 8 (iTBS), 9 (sham), 4 (control); D2: 9, 9, 4; D3: 10, 9, 4; D4: 8, 8, 4; (Ad) D1: 9, 9, 4; D2: 10, 9, 4; D3: 10, 10, 4; D4: 10, 10, 4; (Ba) D1: 8, 9, 4; D2: 10, 9, 4; D3: 9, 9, 4; D4: 8, 9, 4; (Bb) D1: 8, 9, 4; D2: 10, 10, 4; D3: 10, 10, 4; D4: 10, 10, 4.

cell counts was performed in two ways. First, all arcs were normalized to the mean of all contralateral arcs of the entire control group because these counts resemble the normal state. In a second step, we first normalized all individual arcs to the corresponding arcs of the contralateral side in each individual animal to eliminate any effects that might influence both sides as rTMS does (and deafferentation possibly might), aiming to clarify

more specifically any differences between the experimental groups for the experimental hemisphere.

Statistical analysis

Using the Shapiro–Wilk test, we found that most data sets were normally distributed, although often close to the limit. Therefore, we analysed all data sets with both

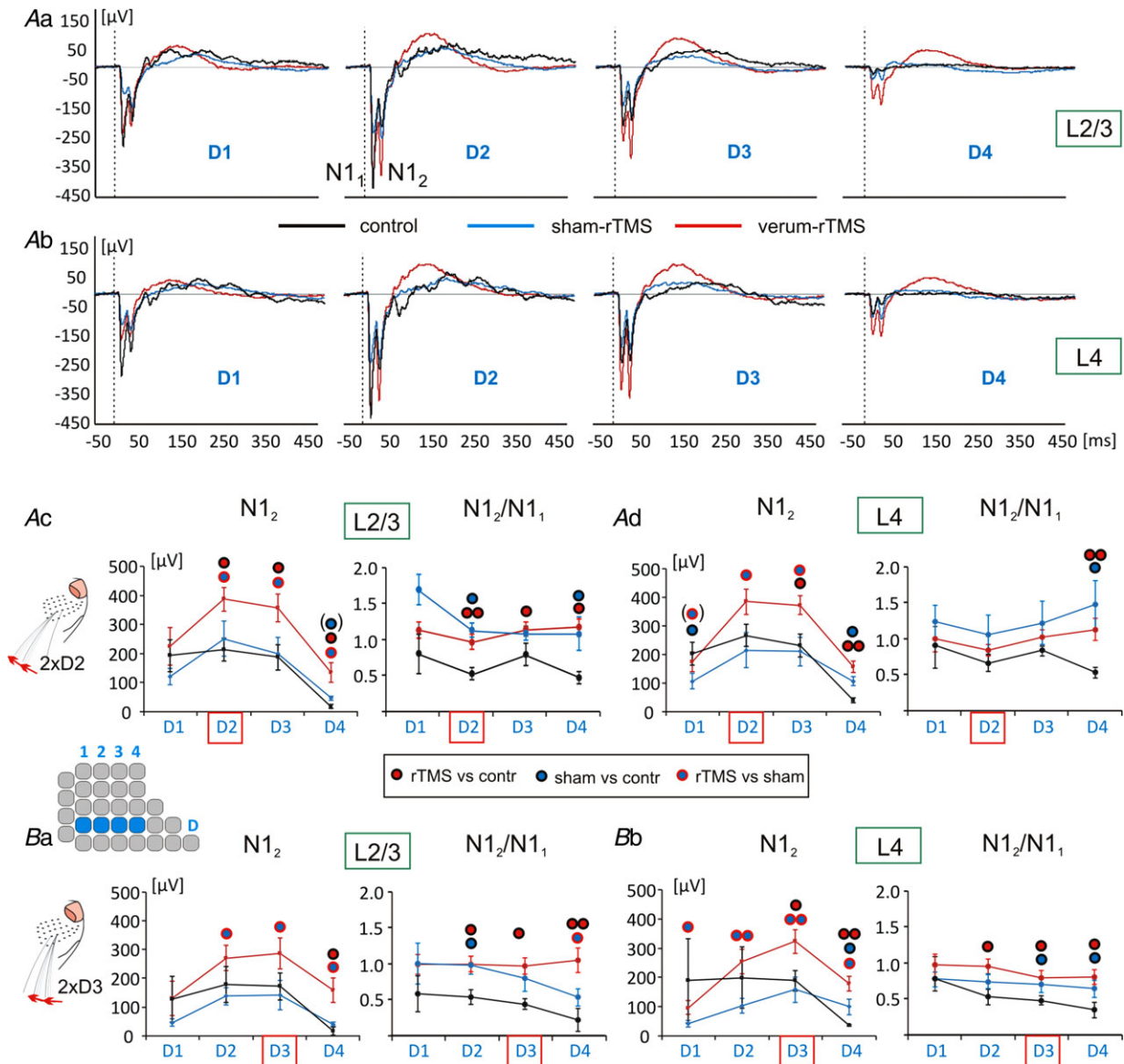


Figure 3. LFP recordings with double stimulation of one whisker and ratio of second to first response amplitude
 Aa and Ab, grand average LFPs evoked with double stimulation of whisker D2 and recordings from the representations of D1–D4 in layer 2/3 (Aa) and layer L4 (Ab) as described in Fig. 2. Statistical analysis of the second response of the LFP component N1 (N1₂, left column) and ratio of second to first response (N1₂/N1₁, right column) for L2/3 (Ac) and L4 (Ad) responses. Ba and Bb, same analysis as in Ac/Ad but with double stimulation of whisker D3. Coloured dots indicate significant differences for pairwise comparison between groups (*U* test); for example, red circle filled blue: sham vs. active rTMS group. Number of dots indicates significance level: 1: $P < 0.05$; 2: $P < 0.01$. Symbols in brackets indicate P values between 0.05 and 0.1 (strong trend). For numbers of animals per dataset, see legend to Fig. 2.

Table 1. Results of ANOVA calculated for changes in N1 and P1 wave with active and sham rTMS treatment of whisker-deafferented animals compared to controls

Stimulated barrel	Layer	LFP wave	Factor	d.f.	F value	P value
D2	L4	N1	TMS	2,90	8.649	<0.001
D2	L2/3	N1	TMS	2,93	9.613	<0.001
D2	L4	P1	TMS	2,90	10.929	<0.001
D2	L2/3	P1	TMS	2,93	14.358	<0.001
D3	L4	N1	TMS	2,93	6.535	0.002
D3	L2/3	N1	TMS	2,83	3.085	0.052
D3	L4	P1	TMS	2,93	17.861	<0.001
D3	L2/3	P1	TMS	2,83	7.555	0.001
D2	L4	N1	BARREL	3,89	13.891	<0.001
D2	L2/3	N1	BARREL	3,92	14.614	<0.001
D2	L4	P1	BARREL	3,89	5.382	0.002
D2	L2/3	P1	BARREL	3,92	8.214	<0.001
D3	L4	N1	BARREL	3,92	14.615	<0.001
D3	L2/3	N1	BARREL	3,82	5.052	0.003
D3	L4	P1	BARREL	3,92	10.552	<0.001
D3	L2/3	P1	BARREL	3,82	5.429	0.002

Only factors TMS and BARREL were included to achieve separate analysis of layers L2/3 and L4. d.f. = degrees of freedom (factor, data). Data obtained with stimulation of either D2 or D3 are from identical sets of animals.

Table 2. Results of ANOVA calculated for changes in N2 amplitude and N₁₂/N₁₁ ratio with active and sham rTMS treatment of whisker-deafferented animals compared to controls

Stimulated barrel	Layer	LFP wave	Factor	d.f.	F value	P value
D2	L4	N2	TMS	2,90	10.078	<0.001
D2	L2/3	N2	TMS	2,84	8.615	<0.001
D2	L4	N ₁₂ /N ₁₁	TMS	2,90	2.833	0.065
D2	L2/3	N ₁₂ /N ₁₁	TMS	2,84	4.510	0.014
D3	L4	N2	TMS	2,89	9.597	<0.001
D3	L2/3	N2	TMS	2,84	8.212	0.001
D3	L4	N ₁₂ /N ₁₁	TMS	2,89	5.727	0.005
D3	L2/3	N ₁₂ /N ₁₁	TMS	2,84	7.721	0.001
D2	L4	N2	BARREL	3,89	12.574	<0.001
D2	L2/3	N2	BARREL	3,84	9.391	<0.001
D2	L4	N ₁₂ /N ₁₁	BARREL	3,89	0.311	0.817
D2	L2/3	N ₁₂ /N ₁₁	BARREL	3,84	0.953	0.42
D3	L4	N2	BARREL	3,88	5.386	0.149
D3	L2/3	N2	BARREL	3,83	4.990	0.003
D3	L4	N ₁₂ /N ₁₁	BARREL	3,88	1.649	0.185
D3	L2/3	N ₁₂ /N ₁₁	BARREL	3,83	1.143	0.337

Only factors TMS and BARREL were included to achieve separate analysis of layers L2/3 and L4. d.f. = degrees of freedom (factor, data). Data obtained with stimulation of either D2 or D3 are from identical sets of animals.

parametric (ANOVA, Tukey's) and non-parametric tests (Whitney–Mann *U* test for independent samples and a Wilcoxon test for dependent samples) and report the lesser statistical outcome for group comparisons, which generally resulted from the non-parametric tests. $P < 0.05$ was considered statistically significant but, because of current discussions regarding how much such a sharp limit is meaningful (Amrhein *et al.* 2019), we also report those with a strong trend ($P < 0.1$). In a few cases, we had to exclude data of LFP components either because they were affected by artefacts or because of too much deviation from the mean ($2.5 \times \text{SD}$). Such outliers were primarily a result of the too small LFP amplitudes obtained from the barrels D1 and D4 as a result of misplacement of the outer electrodes of the array when centring it to barrels D2 and D3. The electrophysiological data sets thus resulted in a minimum of eight and a maximum of 10 animals per barrel recording site (D1–D4) and experimental group (active or sham iTBS) and four data sets for control animals. The number of animals for the data sets representing the number of cells labelled by a distinct marker varied between five and six for the active and sham iTBS groups, as well as four and five in the case of controls (individual slices had to be excluded because not all barrels of interest could be equally well quantified). Numbers of individual data sets are indicated as appropriate and via degrees of freedom for the ANOVA results (Tables 1–4).

Table 3. Results of ANOVA calculated for changes in neuronal marker expression with sham and active rTMS treatment of whisker-deafferented animals compared to controls (factor 1, TMS) and differences between ARCs (factor 2) normalized to contralateral side of the control group

Marker	Layer	Factor	d.f.	F value	P value
c-Fos	L4	TMS	2,71	6.048	0.004
c-Fos	L2/3	TMS	2,82	0.292	0.748
zif268	L4	TMS	2,76	5.572	<0.001
zif268	L2/3	TMS	2,69	2.184	0.12
GAD67	L4	TMS	2,77	14.580	<0.001
GAD67	L2/3	TMS	2,62	3.738	0.031
PV	L4	TMS	2,82	9.817	<0.001
PV	L2/3	TMS	2,87	4.950	0.01
c-Fos	L4	ARCs	4,70	98.851	<0.001
c-Fos	L2/3	ARCs	4,81	21.891	<0.001
zif268	L4	ARCs	4,75	9.358	<0.001
zif268	L2/3	ARCs	4,70	6.752	<0.001
GAD67	L4	ARCs	4,76	0.617	0.652
GAD67	L2/3	ARCs	4,70	0.537	0.709
PV	L4	ARCs	4,81	0.790	0.535
PV	L2/3	ARCs	4,86	0.011	1.000

d.f. = degrees of freedom (factor, data).

Table 4. Results of ANOVA calculated for changes in neuronal marker expression with sham and active rTMS treatment of whisker-deafferented animals compared to controls (factor 1, TMS) and differences between ARCs (factor 2) normalized internally to the contralateral side of individual animals

Marker	Layer	Factor	d.f.	F value	P value
c-Fos	L4	TMS	2,57	0.431	0.653
c-Fos	L2/3	TMS	2,65	3.767	0.029
zif268	L4	TMS	2,61	0.380	0.686
zif268	L2/3	TMS	2,65	2.922	0.062
GAD67	L4	TMS	2,61	10.652	<0.001
GAD67	L2/3	TMS	2,61	2.983	0.062
PV	L4	TMS	2,65	3.767	0.029
PV	L2/3	TMS	2,65	13.955	<0.001
c-Fos	L4	ARCs	3,56	71.584	<0.001
c-Fos	L2/3	ARCs	3,64	31.851	<0.001
zif268	L4	ARCs	3,60	16.395	<0.001
zif268	L2/3	ARCs	3,64	8.343	<0.001
GAD67	L4	ARCs	3,60	1.045	0.381
GAD67	L2/3	ARCs	3,60	0.158	0.924
PV	L4	ARCs	3,64	0.286	0.835
PV	L2/3	ARCs	3,64	0.032	0.992

d.f. = degrees of freedom (factor, data).

In the case of the histological data, ANOVA was applied with the factors TMS (active, sham, control), ARCs (see grouping above) and LAYER (L2/3 vs. L4) followed by a *post hoc* Tukey's test and pairwise comparison with either Whitney–Mann *U* or Wilcoxon test. In the case of the LFP data, the amplitudes of the different LFP components (N1, P1 and N₁₂ in the case of double stimulation) and the ratio of N₁₂/N₁₁ were analysed using ANOVA with factors TMS, BARREL (D1, D2, D3 and D4) and LAYER followed by Tukey's test (and *U* test or Wilcoxon test). Furthermore, we performed a correlation analysis according to Pearson correlation coefficient with a matrix comparing the LFP components N1, P1 and ratio of second-to-first N1 amplitude (N₂/N₁) when using double stimuli for all of the responses recorded from L2/3 or L4 and with either whisker D2 or D3 stimulated. In a similar fashion, we established correlation matrices for the numbers of labelled cells counted in different layers and different arcs. We then compared matrices prepared for the different experimental groups (controls, sham- and active-rTMS). All statistical tests were conducted using SPSS, version 25 (IBM Deutschland GmbH, Ehningen, Germany).

Results

LFPs

Local field potentials simultaneously recorded from barrels D1 to D4 (first L2/3 then L4) showed a sharp

early negative wave (N1) followed by a smaller and longer lasting positive wave (P1). The amplitude of N1 was always highest within the barrel corresponding to stimulation of the principal whisker (the primary input whisker), which was either D2 or D3; example curves for D3 stimulation are shown in Fig. 2Aa,b. Neighbouring barrels showed a smaller N1 size with a steeper decline towards rostral (D4) than caudal barrels (D1). Also, the smaller P1 wave showed an asymmetric decline towards neighbouring barrels. It was of similar size in D2 and D3 when stimulating whisker D3, although clearly smaller in D3 when stimulating whisker D2.

Rats with all whiskers of the left pad plucked except for arcs no. 2 & 3 exhibited a significant reduction of the N1 and P1 wave in L4 and L2/3 when pre-treated with sham rTMS, whereas active rTMS increased the N1 and P1 amplitude back to or even above the control level. ANOVA performed with factors TMS (controls, sham-, active-rTMS), BARREL (D1–D4) and LAYER (L2/3, L4) revealed a significant effect of factors TMS and BARREL for all comparisons (except for one case). The results of ANOVAs separately calculated for the N1 and P1 components for the recordings from the different layers and for the cases with D2 and D3 stimulation are listed in Table 1. Factor LAYER had no effect and also showed no significant interaction with the other factors. Also, the interaction of factors TMS and BARREL was not significant, obviously because the total response amplitudes strongly differed between barrels, whereas the relative effect of TMS was similar. In most cases, *post hoc* Tukey's and Mann–Whitney *U* tests revealed significant differences between active and sham rTMS groups and between sham and control groups for the comparison of N1 and P1 amplitudes. Only rostral barrels showed enhanced LFP amplitudes also for the active rTMS group compared to controls (Fig. 2).

The increase in N1 and P1 amplitudes following active rTMS appeared to abolish the asymmetry in rostral vs. caudal transmission of activity. Because this asymmetry of lateral spread of activity probably relates to an asymmetry of lateral inhibition (see below), we applied the double-stimulation paradigm to the spared whiskers D2 and D3.

Suppression of the second response, if two stimuli are applied to the same whisker at short intervals (i.e. 20 ms), is considered to depend on cortical inhibition (see Discussion). As found in prior studies, the ratio of the second response (N₁₂) to the first (N₁₁) varied on average from 0.5 to 0.8 but was always below 1.0 in all barrels (Fig. 3). This ratio (N₁₂/N₁₁) significantly increased to 1.0, or even higher, with whisker deafferentation and with active iTBS. However, the reason for this change was different for the two experimental conditions. In deafferented animals (sham rTMS), it is related to a decrease in N₁₁ response (Fig. 2), whereas N₁₂ is almost

at control size (Fig. 3). By contrast, in the active rTMS treated animals, $N1_1$ is close to control amplitudes but $N1_2$ is significantly increased above control level.

ANOVA calculated for changes in $N1_2$ amplitude and the $N1_2/N1_1$ ratio with factors TMS and BARREL revealed a significant effect of factor TMS for all cases compared (except for one case; see Table 2). Factor BARREL yielded no significant effect in the case of the $N1_2/N1_1$ ratio because all barrels were affected in a similar manner. Nevertheless, rostral barrels showed a stronger (significant) increase in $N1_2$ amplitude and $N1_2/N1_1$ ratio with active rTMS compared to caudal barrel D1 (see individual data of *post hoc U* test, as indicated in Fig. 3).

Immunohistochemical findings

The electrophysiological data showed that deafferentation and rTMS affected not only principal cortical response amplitudes to whisker stimulation (non-deafferented D2 and D3), but also the lateral spread of activity to neighbouring (deafferented) whisker representations. To clarify whether this was also reflected by regional changes in the expression of neuronal markers resembling either general activity (mostly excitatory, c-Fos, zif268) or inhibitory activity (GAD67, PV), we selectively stimulated one arc (no. 2) and separately analysed arcs of the barrel fields according to experimental conditions, meaning stimulated or not, previously deafferented or not, and either directly neighbouring the non-deafferented arcs or being more distant. Because we found no principal differences in marker expression between arcs that were not stimulated, regardless of being close or far to the stimulated arc, we pooled these groups and distinguished only between the stimulated arc on the deafferented side, the pooled non-stimulated other arcs and the stimulated arcs of the contralateral side in Figs 4 and 5.

Below, we present two different ways of comparing the neuronal marker expression (number of labelled cells) between the different arcs. In a first step, all cell counts were normalized to the grand average of the contralateral barrel field of the entire control group (standard control, step 1). In a second step, we performed an internal normalization before averaging the data by normalizing cell counts of the individual arcs of the deafferented side to the corresponding arcs of the non-manipulated contralateral barrel cortex in individual animals (step 2). The latter would probably reduce the intra-individual differences between hemispheres principally resulting from the inter-individual variability of cell numbers.

Normalization to standard control (step 1)

Expression of the immediate early gene product c-Fos showed a strong dependence on prior whisker activation

in all groups. Accordingly, ANOVA revealed a strong dependence on factor ARCs (for all comparisons conducted, see Table 3). Barrels corresponding to the arc directly activated during exploration by the spared whiskers (arc no. 2, A2–E2) showed $1.5\times$ to $2.5\times$ higher numbers of c-Fos positive cells in L4 compared to the contralateral hemisphere of the control group (Wilcoxon: $P < 0.05$ for all the three groups) (Fig. 4Bb), whereas the difference was smaller in L2/3 (+20%) but significant (Fig. 4Ba). Correspondingly, factor LAYER of ANOVA test showed a significant effect ($P < 0.002$) and a significant interaction with factor TMS ($P < 0.001$) in this case.

The group of barrels of the deafferented side being not stimulated showed less than 50% of control values in L4 and between 40% and 60% in L2/3 (all cases with $P < 0.05$). No significant differences were found between the three experimental groups, except for the sham group, which had significantly lower c-Fos+ cells within the stimulated arc of L4 compared to the active rTMS and control group, and also ANOVA reported a significant effect of factor TMS. The data of this step of the analysis (step 1) with normalization to the grand average of the contralateral side of the control animals are represented by the left groups of bars in Fig. 4Ba,b.

Differences in the number of zif268 positive cells regarding the different arcs were less strong compared to c-Fos labelling. Nevertheless, ANOVA revealed a significant effect of factor ARCs for L4 and L2/3 (Table 3) and the stimulated barrels of arc no. 2 showed significantly higher numbers of zif268+ cells than the non-stimulated arcs (L4, L2/3) (Fig. 4Ca,b); however, their number did not increase above the level of the contralateral control side. Deafferented arcs showed lowered numbers of zif268+ cells both in L4 and L2/3, although these were significantly different from the control side ($P < 0.05$) in only a few cases (left groups of bars in Fig. 4Ca,b). Also, in this case, the sham-rTMS group showed lower numbers of labelled cells and ANOVA revealed a significant effect of factor TMS for L4 (Table 3).

In the case of GAD67, the active- and sham-rTMS groups showed enhanced numbers of labelled cells within L4 that were statistically different from the corresponding arcs of the control group (left groups of bars in Fig. 5Ba,b). ANOVA reported a significant effect of factor TMS for L4 and L2/3 (Table 3), although no significant differences were found for layer L2/3 on the basis of individual arcs. Within L4, the sham-rTMS group showed a higher number of GAD67+ cells compared to the active group, although the differences were not statistically significant. Factor ARCs was not significant, indicating that all barrels were affected in a similar fashion.

In the case of PV, almost all barrels within L4 of the deafferented experimental side showed an increased number of PV+ cells in the active group compared to the control group (Fig. 5Ca,b), whereas, in L2/3,

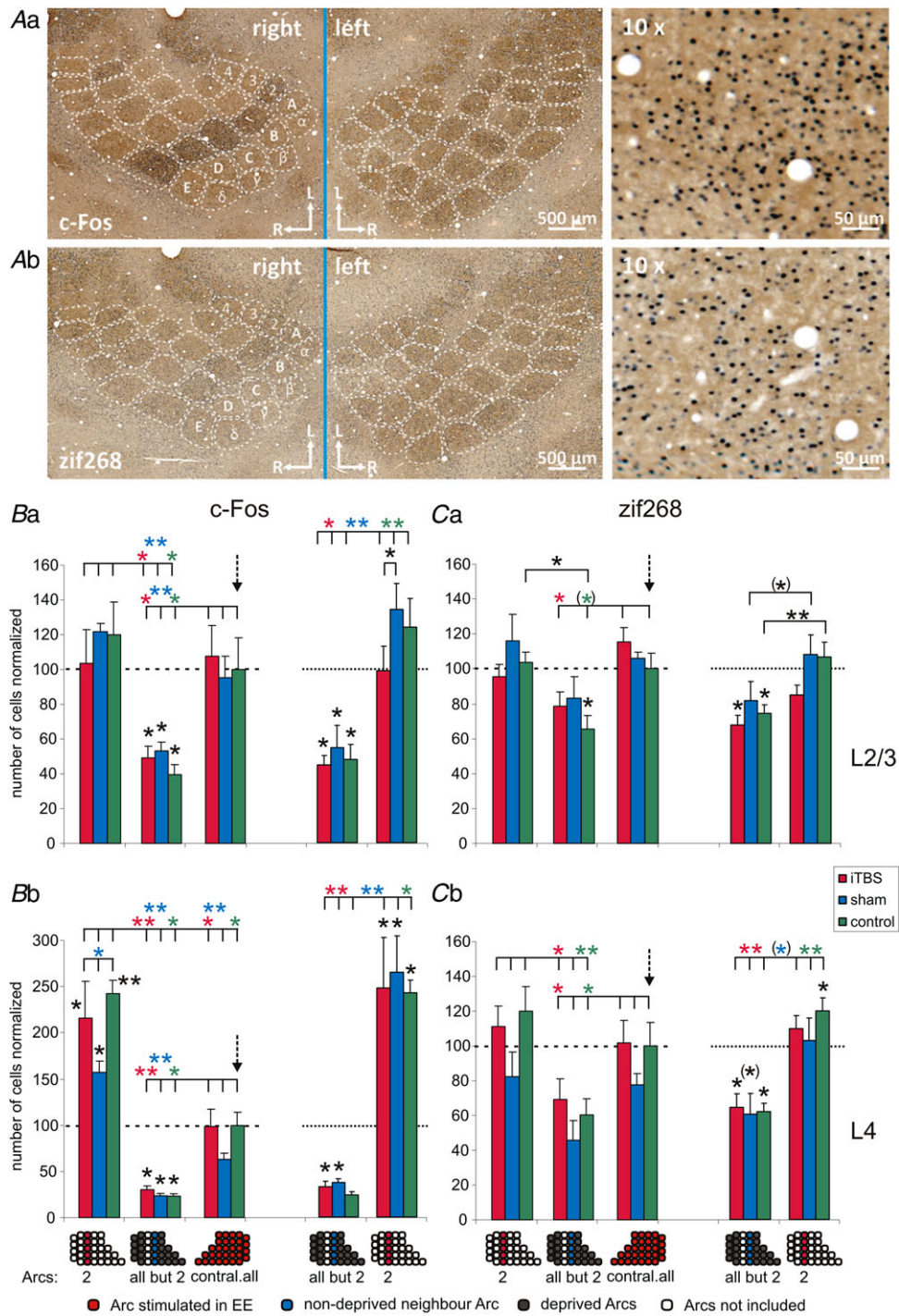


Figure 4. c-Fos and zif268 expression in the left and right barrel fields
Aa and *Ab*, examples of right (experimental) and left (contralateral) barrel field at L4 with c-Fos+ and zif268+ neurons after stimulation of the whiskers of arc no. 2 prior to immunohistochemistry. Enlarged (10x) view of labelled cells to the right. Individual barrels are outlined by dotted lines and labelled A–E and (2–4) according to rows and arcs, respectively. Greek letters indicate barrels corresponding to the caudally located straddlers. *Ba*, *Bb*, *Ca* and *Cb*, number of c-Fos+ (*B*) and zif268+ (*C*) neurons in layers 2/3 (upper) and L4 (lower) counted in different arcs. The three groups of bars to the left show cell numbers normalized to the grand average of the contralateral barrel field of the control rats (see arrows and dotted lines). The two groups of bars to the right show cell numbers after internal normalization to the corresponding contralateral arcs in each individual before averaging. The left

only the contralateral hemisphere exhibited significantly enhanced numbers of PV+ cells compared to controls and sham-controls. ANOVA revealed a significant effect of factor TMS for L4 and L2/3 but no effect of factor ARCs (Table 4).

In the case of zif268, GAD67 and PV analysis, factor LAYER included in ANOVA did not show a significant effect and did not show significant interactions with factors TMS and ARCs.

Internal normalization of arc data to contralateral control side (step 2)

Internal normalization of cell counts obtained from the deafferented barrel cortex with reference to the contralateral barrel cortex yielded to partially different results. Changes in the number of c-Fos+ and zif268+ cells per arcs of interest were principally similar to the normalization of step 1 (compare right groups of bars in each diagram of Fig. 4 with those to the left). ANOVA revealed a significant difference for ARCs for both markers and both layers, whereas factor TMS was relevant only for c-Fos in L4 (Table 5).

GAD67+ and PV+ cells now showed proportionally different changes (right groups of bars in diagrams of Fig. 5). In L4 but not in L2/3, the sham-rTMS group showed enhanced numbers of GAD67+ cells. ANOVA reports a highly significant effect of factor TMS (Table 4). On the other hand, no significant differences between groups and arcs were found for the number of PV+ cells in L4 but a significantly higher number of PV+ cells for the sham-rTMS group in L2/3 compared to the active-rTMS group (factor TMS highly significant) (Table 4). Factor ARCs was neither significant for GAD67 or PV, nor for L4 or L2/3, indicating that all barrels were affected in a similar fashion.

Correlation analysis of LFP components and neuronal activity markers

To identify relationships between changes in LFP components, we calculated correlation matrices comparing the amplitudes of the N1 and P1 responses and the ratio of the second to the first N1 response with double stimulation (N2/N1) for responses obtained

from the different layers and with either D2 or D3 stimulation. Table 5 lists those cases with significant correlations, grouped by categories as within or across layer correlations.

Positive correlations between the amplitudes of N1 and P1 responses could be expected if the signals originated from the same or different cortical layer belonging to the same cortical column because these signals are directly coupled by local neuronal processes. Also, positive correlations across different arcs, if stimulated either at whisker D2 or D3, could be expected as a result of a similar responsiveness and lateral spread of activity. The three experimental groups showed some but no principal difference in this respect. However, one obvious change for the active-rTMS group was the occurrence of negative correlations between N1 or P1 amplitudes and the N2/1 ratio (see cases 5–10, 13, 19, 23, 24 and 36 of Table 5; cases 5 and 7 are shown in Fig. 6). This appeared to be a sign of altered inhibition after iTBS, probably that of the recurrent type, which could mediate the suppression of the second response. In other cases, primarily in the control group, a positive correlation was found between this ratio and N1 and P1.

In a similar way, we also compared the numbers of cells labelled for the different neuronal activity markers, by differentiating between the layers L2/3 and L4 and further between the arcs of the deafferented barrel field that had been stimulated (S) or not (NS) and the averages of complete contralateral barrel field (C) as in the analyses shown before. Table 6 lists the significant cases also in a categorized manner.

Many positive correlations for the same marker are evident across arcs (S, NS, C) for the same layer irrespective of the experimental group. However, the active-rTMS group shows some more positive correlations for c-Fos and PV in this category but less for zif268 (cases 3–18). Most strikingly, the sham-rTMS group showed a number of positive correlations for the number of PV+ cells when compared across layers and arcs (cases 19–22; see also Fig. 7, left) but a negative correlation between c-Fos and PV (cases 38–40; Fig. 7, middle), indicating that deafferentation might induce a more equal distribution of marker activity within the barrel field with an increased ratio of inhibition (PV) vs. excitation (c-Fos). By contrast, the active-rTMS group showed negative correlations between zif268 and PV (cases 44–46; Fig. 7, right) that

bars of each group show the results for arc 2 of the deafferented side that had been stimulated in EE. The next group of bars to the right shows averaged cell numbers for the arcs of the deafferented side that had not been stimulated. The group in the middle shows the averaged cell numbers for the complete contralateral barrel field. Black asterisks directly above columns indicate significant differences (*U* test) to the contralateral barrel field of the control group (indicated by the dotted line); asterisks above the horizontal lines indicate significant differences between either the stimulated arc and all other arcs, or between contralateral barrels and all non-stimulated arcs (Wilcoxon test). Colour indicates the experimental groups compared (green, controls; blue, sham rTMS; red, active iTBS) **P* < 0.05, ***P* < 0.01. Number of animal included per data set: (Ba) 6 (iTBS), 6 (sham), 5 (control); (Bb) 5, 6, 4; (Ca) 6, 6, 5; (Cb) 5, 6, 5.

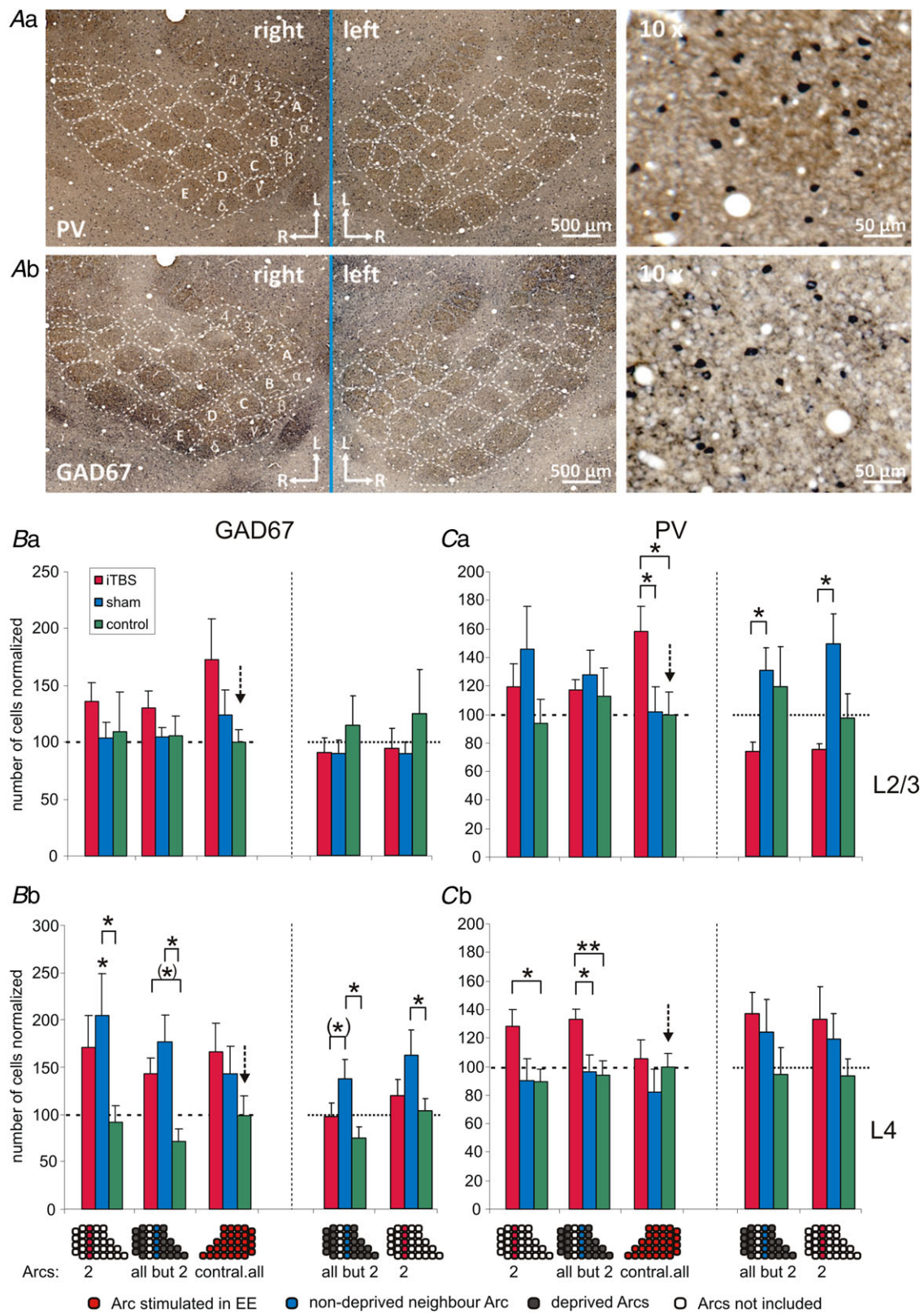


Figure 5. GAD67 and PV expression in the left and right barrel fields
 Aa and Ab, examples of right (experimental) and left (contralateral) barrel field at L4 with GAD67+ and PV+ neurons after stimulation of the whiskers of arc no. 2 prior to immunohistochemistry. Enlarged (10x) view of labelled to the right. Individual barrels are outlined by dotted lines and labelled A–E and (2–4) according to rows

were not evident in the other groups, which showed, by trend, positive correlations. The negative correlation between zif268+ (needed for LTP persistence, Abraham *et al.* 1993) and PV+ cells (inhibition) fits well with the concept of disinhibition needed to allow plastic processes (Froemke *et al.* 2015; Letzkus *et al.* 2015).

The computational model

To support our conclusions regarding the neuronal network mechanisms contributing to the effects of sensory deafferentation and the opposing effects of iTBS-rTMS, we established a simple computational model (Fig. 8). In particular, we wanted to confirm whether an asymmetric rostro-caudal inhibition between barrels can replicate the LFP amplitudes resulting from the lateral spread of activity and the changes induced by iTBS-rTMS as a result of a possible disinhibitory effect. The model includes the four barrels, D1 to D4, an afferent input (which would be thalamocortical to L4, or L4 to L2/3 projection), including feed-forward inhibition (via the red neurons), lateral excitatory projections from pyramidal neurons (green) to pyramidal neurons and inhibitory neurons of the neighbouring barrels, and lateral feed-forward inhibition (red) within the barrels. The lateral inhibition was set either asymmetric towards rostral direction according to the findings discussed above, or symmetrical.

A program written in Visual Studio (Microsoft Corp. Redmond, WA, USA) allowed the combination of three different connection modes: (i) symmetric and equal lateral excitation across all barrels *vs.* a different connection strength between D2 and D3 (the spared barrels) and the further projection to D1 and D4; (ii) symmetric *vs.* asymmetric lateral inhibition; and (iii) recurrent inhibition on or off. The latter was needed only in case of simulating the second N1 response with double stimulation. The program performed an iterative fitting procedure of the experimental data (both sets with either D2 or D3 stimulation were calculated always with the same settings) (Fig. 8) by changing the level of lateral excitation and feed-forward inhibition with two nested loops to achieve least mean square differences (MSqD). In a first step, we fitted the N1 responses to D2 and D3 stimulation (single stimulus) of barrels D1–D4 for the control conditions (Fig. 8*Aa,b*). It was revealed that

the modes equal lateral excitation and asymmetric lateral inhibition fitted the data with the lowest MSqD. In this case, lateral excitation had a strength of 70% and that of feed-forward inhibition was 40%, resulting in a total level of 28% inhibition with 70% input drive. To achieve a value of 100% response amplitude for the directly stimulated barrel (D2 or D3), as a result of normalization of the data to this reference, the thalamic drive had to be 167% to overcome the 40% of feed-forward inhibition.

The drop of LFPs amplitude of the principal barrel with deafferentation (sham-rTMS condition) was simulated by reducing the responsiveness of this barrel to the afferent input from 100% to 60% at the same time as keeping feed-forward inhibition strength at 40% of excitation (Fig. 8*Ba,b*). The data of the other barrels could be best fit by the modes asymmetric lateral inhibition but unequal lateral excitation. The excitatory connectivity between the spared barrels D2 and D3 had to be increased from 70% to 90% and the transmission further to D1 and D4 decreased from 70% to 50%. The level of lateral inhibition remained at 40% for this fit. This scenario would resemble potentiation of connections between barrels related to the spared whiskers and a depression of the deafferented barrels as discussed above.

The data obtained with active iTBS could be best fitted with the same excitatory lateral spread as in case of deafferentation (sham-rTMS condition) but with a reduction in feed-forward inhibition from 40% to 20%. In addition, a small increase in afferent responsiveness from 100% to 112% was required to achieve the 90% response level of the thalamic input barrels D2 or D3, respectively (Fig. 8*Ca,b*). In summary, this simple model shows that the change in lateral spread of activity from the principal barrel over one to two neighbouring barrels could indeed be replicated by an asymmetric lateral inhibition. Moreover, sensory deafferentation effects were best explained by a general depression of barrel field responsiveness but, additionally, a pairing effect of the two spared arcs based on enhanced strength of reciprocal connectivity.

The disinhibitory effect of iTBS-rTMS not only enhanced response amplitudes back to control level, but also increased the responses of rostral barrels even stronger, leading to a loss of asymmetric inhibition as found with the experimental data. This is in accordance with our previous findings indicating that iTBS-rTMS induces cortical disinhibition, with reduced numbers of

and arcs, respectively. Greek letters indicated barrel corresponding to the caudally located straddlers. *Ba*, *Bb*, *Ca* and *Cb*, number of GAD67+ (*B*) and PV+ (*C*) neurons in layers 2/3 (upper) and L4 (lower) counted in different arcs. As in Fig. 4, the three groups of bars to the left show cell numbers normalized to the grand average of the contralateral barrel field of the control rats (arrows, dotted lines). The two groups of bars to the right show cell numbers after internal normalization to the corresponding contralateral arcs in each individual before averaging. Otherwise same arcs were analysed as shown in Fig. 4. Black asterisks directly above columns indicate significant differences (*U* test) to the contralateral barrel field of the control group (indicated by the dotted line); asterisks above horizontal lines indicate significant differences between experimental groups (*U* test). **P* < 0.05, ***P* < 0.01. For numbers of animals per data set, see legend to Fig. 4.

Table 5. Significant cases of the Pearson correlation matrices obtained by comparing N1, P1 and ratio of second and first N1 response (N2/1) for different layers (L23, L4) and different whisker stimulation (D2, D3)

No.	X	vs.	Y	Active rTMS		Sham rTMS		Controls	
				r value	P value	r value	P value	r value	P value
Same barrel - same layer									
1	N1_D2_L23	vs.	P1_D2_L23	0.842**	<0.001	.670**	<0.001	0.622*	0.01
2	N1_D2_L4	vs.	P1_D2_L4	0.634**	<0.001	.723**	<0.001	0.598*	0.014
3	N1_D3_L4	vs.	P1_D3_L4					0.758**	0.001
4	N1_D3_L23	vs.	N2/1_D3_L23					0.651**	0.006
5	N1_D2_L23	vs.	N2/1_D2_L23	-0.432*	0.011				
6	P1_D2_L23	vs.	N2/1_D2_L23	-0.446**	0.008				
7	N1_D2_L4	vs.	N2/1_D2_L4	-0.386*	0.017				
8	P1_D2_L4	vs.	N2/1_D2_L4	-0.465**	0.003				
9	N1_D3_L4	vs.	N2/1_D3_L4	-0.481**	0.003				
10	P1_D3_L4	vs.	N2/1_D3_L4	-0.439**	0.007				
Same barrel - across layers									
11	N1_D2_L23	vs.	N1_D2_L4	0.863**	<0.001	0.769**	<0.001	0.931**	<0.001
12	N1_D2_L23	vs.	P1_D2_L4	0.618**	<0.001			0.734**	0.001
13	N1_D2_L23	vs.	N2/1_D2_L4	-0.417*	0.013				
14	N1_D3_L23	vs.	N1_D3_L4	0.849**	<0.001	.790**	<0.001		
15	N1_D3_L23	vs.	P1_D3_L4	0.484**	0.003	.733**	<0.001		
16	N1_D3_L23	vs.	N2/1_D3_L4			-0.352*	0.038	0.534*	0.033
17	P1_D2_L23	vs.	P1_D2_L4			0.371*	0.026	0.844**	<0.001
18	P1_D2_L23	vs.	N1_D2_L4			0.470**	0.004		
19	P1_D2_L4	vs.	N2/1_D2_L23	-0.381*	0.024				
20	P1_D3_L23	vs.	N1_D3_L4	0.454**	0.006	0.671**	<0.001	0.553*	0.026
21	P1_D3_L23	vs.	P1_D3_L4			0.755**	<0.001	0.862**	<0.001
22	N2/1_D2_L23	vs.	N2/1_D2_L4	0.739**	<0.001	0.458**	0.005	1.000**	<0.001
23	N2/1_D3_L23	vs.	N1_D3_L4	-0.370*	0.029				
24	N2/1_D3_L23	vs.	P1_D3_L4	-0.387*	0.021				
25	N2/1_D3_L23	vs.	N2/1_D3_L4	0.508**	0.002	0.361*	0.03	0.868**	<0.001
Same layer – across barrels									
26	N1_D2_L4	vs.	N1_D3_L4	0.405*	0.012	0.407*	0.011	0.575*	0.02
27	N1_D2_L23	vs.	N1_D3_L23	0.620**	<0.001	0.535**	0.001	0.788**	<0.001
28	N1_D2_L23	vs.	P1_D3_L23	0.785**	<0.001	0.640**	<0.001		
29	N1_D2_L4	vs.	P1_D3_L4	0.379*	0.019				
30	N1_D2_L4	vs.	N2/1_D3_L4					0.659**	0.005
31	N1_D2_L23	vs.	N2/1_D3_L23					0.703**	0.002
32	P1_D2_L23	vs.	N1_D3_L23			0.351*	0.039		
33	P1_D2_L23	vs.	P1_D3_L23			0.474**	0.004		
34	P1_D2_L23	vs.	P1_D3_L23			0.433**	0.007	0.762**	0.001
35	P1_D2_L4	vs.	P1_D3_L4	0.332*	0.042			0.703**	0.002
36	P1_D3_L23	vs.	N2/1_D2_L23	-0.383*	0.025				
37	N2/1_D2_L4	vs.	P1_D3_L4	0.339*	0.035				
38	N2/1_D2_L23	vs.	N2/1_D3_L23	-0.356*	0.039	0.403*	0.015	-0.502*	0.048
39	N2/1_D2_L4	vs.	N2/1_D3_L4			-0.445**	0.005	-0.550*	0.027
Across barrels – across layers									
40	N1_D3_L23	vs.	N1_D2_L4	0.470**	0.004			0.784**	<0.001
41	N1_D3_L23	vs.	P1_D2_L4					0.502*	0.048
42	N1_D2_L23	vs.	N1_D3_L4	0.339*	0.046	0.446**	0.006		
43	N1_D2_L23	vs.	P1_D3_L4			0.546**	0.001		
44	N1_D2_L23	vs.	N2/1_D3_L4					0.540*	0.031
45	N1_D2_L4	vs.	N2/1_D3_L23					0.716**	0.002
46	P1_D3_L23	vs.	N1_D2_L4	0.521**	0.001	0.390*	0.021		
47	P1_D3_L23	vs.	P1_D2_L4	0.473**	0.004			0.741**	0.001
48	P1_D2_L23	vs.	P1_D3_L4					0.661**	0.005

(Continued)

Table 5. Continued

No.	X	vs.	Y	Active rTMS		Sham rTMS		Controls	
				r value	P value	r value	P value	r value	P value
49	N2/1_D2_L23	vs.	P1_D3_L4	0.382*	0.024				
50	N2/1_D2_L23	vs.	N2/1_D3_L4	-0.408*	0.017			-0.550*	0.027
51	N2/1_D3_L23	vs.	N2/1_D2_L4	-0.394*	0.019	-0.405*	0.014	-0.502*	0.048

Such matrices were established for the active-rTMS, sham-rTMS and control groups. Negative correlations are indicated in bold.

GAD67+ and PV+ cells (Trippe *et al.* 2009; Mix *et al.* 2010; Benali *et al.* 2011; Hoppenrath & Funke, 2013; Volz *et al.* 2013) and increased sensory responsiveness of rat barrel cortex (Thimm & Funke, 2015).

To further test whether iTBS-rTMS affected cortical inhibition, we applied the double stimulation protocol. Therefore, we simulated also this scenario by introducing recurrent inhibition into the model (orange neurons) (Fig. 9). To reduce complexity, afferent feed-forward inhibition is not shown here but is the same as in the model described above. The model now shows the situation for the second response (N1₂) with recurrent inhibition now active as a result of the first response. As with lateral inhibition, a fraction of 40% inhibition of the 70% of excitatory drive (yielding 28% effective inhibition) best fitted the amplitude of the second response in all the four barrels with all other settings unchanged.

The strength of recurrent inhibition actually dropped to almost to zero to fit the experimental data during the deafferented condition with active rTMS (Fig. 9C). The results were less clear in case of deafferentation but with sham rTMS. Recurrent inhibition within the spared barrels D2 and D3 had to be reduced to almost zero to

fit the data but had to be kept at the previous level of 40% to best fit the data of D1 and D4. Obviously, reduced afferent responsiveness led to a reduced drive of recurrent inhibition, although an additional amount of reduced inhibition appeared to be necessary to complement the experimental data. The latter was probably the result of stronger pairing effects between the spared arcs. In the case of active iTBS, a general shut-down of recurrent inhibition across all barrels appears to be the most plausible explanation, considering that experimental data showed a ratio of second to first response amplitude close to 1.0. In a previous study based on multi-unit spiking activity and acute administration of iTBS-rTMS, we also found a strong increase in this ratio (from 0.17 to 0.75) (Thimm & Funke, 2015).

Discussion

Summary of major findings

Partial deafferentation of the left whisker pad by removing all whiskers except arcs no. 2 & 3 led to an overall reduction of evoked sensory response amplitudes in the right barrel

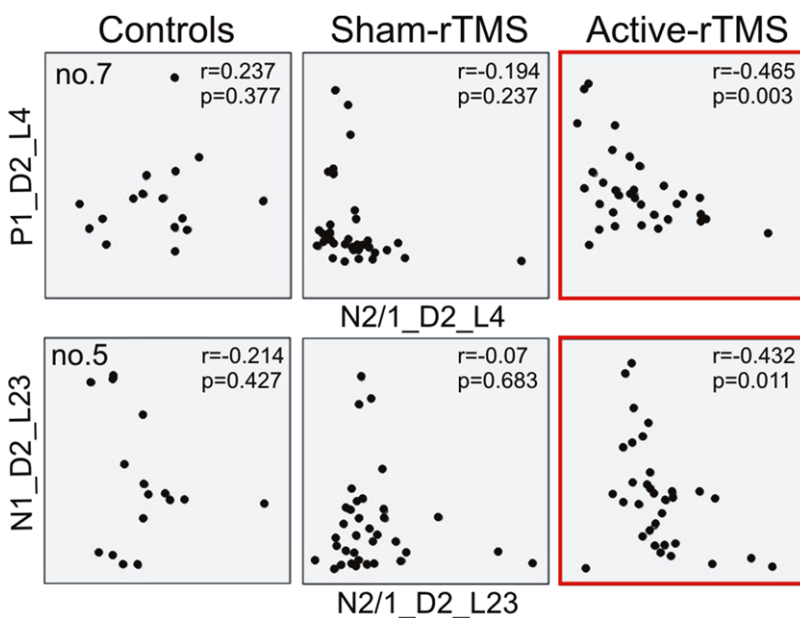


Figure 6. Correlations of LFP components N1 and P1 and ratio N2/1

Two cases (5 and 7 of Table 5) are shown in which the N1 responses recorded from layers 2/3 (L23) and P1 recorded from L4, both with D2 stimulation, show a negative correlation to the N2/1 ratio in the group receiving active rTMS (red frames). No such correlation was found in the control and sham-rTMS groups.

Table 6. Significant cases of the Pearson correlation matrices obtained by comparing cells labelled for c-Fos (cFos), zif268 (zif), GAD67 and PV for different layers (L23, L4) and the arcs of the deafferented side which had been stimulated (S) or not (NS) or those of the complete contralateral side (C)

No.	X	vs.	Y	Active rTMS		Sham rTMS		Controls	
				r value	P value	r value	P value	r value	P value
Same marker – same arc – across layers									
1	PV_C.L4	vs.	PV_C.L23	0.926**	0.008				
2	zif_C.L4	vs.	zif_C.L23					0.900*	0.037
Same marker – same layer – across arcs									
3	cFos_S.L23	vs.	cFos_NS_23	0.956**	0.003			0.945*	0.015
4	cFos_C.L23	vs.	cFos_NS_23	0.823*	0.044				
5	cFos_S.L4	vs.	cFos_NS.L4	0.936*	0.019				
6	zif_S.L23	vs.	zif_NS.L23	0.889*	0.018	0.995**	<0.001		
7	zif_S.L4	vs.	zif_NS.L4	0.978**	0.004	0.816*	0.048	0.924*	0.025
8	zif_C.L4	vs.	zif_S.L4	0.904*	0.035			0.882*	0.048
9	zif_C.L23	vs.	zif_NS.L23			0.927**	0.008		
10	zif_C.L23	vs.	zif_S.L23			0.942**	0.005		
11	zif_C.L4	vs.	zif_NS.L4					0.943*	0.016
12	GAD67_S.L23	vs.	GAD67_NS.L23	0.854*	0.03	0.987**	0.002	0.996**	<0.001
13	GAD67_S.L4	vs.	GAD67_NS.L4	0.919**	0.01	0.971**	0.006		
14	GAD67_C.L4	vs.	GAD67_S.L4					0.920*	0.027
15	PV_S.L23	vs.	PV_NS.L23	0.903*	0.014	0.993**	<0.001	0.968**	0.007
16	PV_C.L23	vs.	PV_S.L23	0.896*	0.016				
17	PV_C.L23	vs.	PV_NS.L23	0.853*	0.031				
18	PV_S.L4	vs.	PV_NS.L4	0.950**	0.004	0.987**	<0.001	0.990**	0.001
Same marker – across layers – across arcs									
19	cFos_S.L4	vs.	cFos_C.L23			0.930**	0.007		
20	PV_NS.L4	vs.	PV_S.L23			0.815*	0.048		
21	PV_S.L4	vs.	PV_NS.L23			0.843*	0.035		
22	PV_S.L4	vs.	PV_S.L23			0.876*	0.022		
cFos-vs-zif268 – same layer – same arc									
23	cFos_S.L23	vs.	zif_S.L23	0.887*	0.018				
24	cFos_C.L4	vs.	zif_C.L4			0.854*	0.03		
cFos-zif268 – same layer – across arcs									
25	cFos_C.L23	vs.	zif_NS.L23	0.930**	0.007				
26	cFos_NS_23	vs.	zif_S.L23	0.887*	0.019				
cFos-zif268 – across layers – across arcs									
27	cFos_S.L23	vs.	zif_C.L4			-0.917**	0.01		
cFos-GAD67 – same layer – across arcs									
28	cFos_C.L23	vs.	GAD67_NS.L23	0.885*	0.019				
cFos-GAD67 – across layers – same arc									
29	cFos_NS.L4	vs.	GAD67_NS.L23	0.914*	0.03				
30	cFos_C.L23	vs.	GAD67_C.L4	0.828*	0.042				
31	cFos_NS_23	vs.	GAD67_NS.L4	0.849*	0.032				
cFos-GAD67 – across layers – across arcs									
32	cFos_S.L23	vs.	GAD67_NS.L4	0.830*	0.041				
33	cFos_NS_23	vs.	GAD67_C.L4	0.930**	0.007				
34	cFos_S.L23	vs.	GAD67_C.L4	0.868*	0.025				
cFos-PV – same layer – same arc									
35	cFos_C.L4	vs.	PV_C.L4					0.986*	0.014
36	cFos_NS_23	vs.	PV_NS.L23			-0.870*	0.024		
cFos-PV – across layers – across arcs									
37	cFos_NS_23	vs.	PV_C.L4	0.849*	0.032				
38	cFos_NS_23	vs.	PV_S.L23			-0.842*	0.036		
39	cFos_NS_23	vs.	PV_NS.L4			-0.825*	0.043		
40	cFos_NS_23	vs.	PV_S.L4			-0.851*	0.032		

(Continued)

Table 6. Continued

No.	X	vs.	Y	Active rTMS		Sham rTMS		Controls	
				r value	P value	r value	P value	r value	P value
41	cFos_NS_L4	vs.	PV_C_L23					0.971*	0.029
zif268-PV – same layer – same arc									
42	zif_C_L23	vs.	PV_C_L23			0.815*	0.048		
zif268-PV – across layers – across arcs									
43	zif_C_L23	vs.	PV_C_L4	0.823*	0.044				
44	zif_NS_L4	vs.	PV_NS_L23	-0.997**	<0.001				
45	zif_NS_L4	vs.	PV_S_L23	-0.925*	0.024	0.895*	0.04		
46	zif_S_L4	vs.	PV_NS_L23	-0.984**	0.002	0.891*	0.043		
47	zif_S_L4	vs.	PV_S_L23			0.962**	0.009		
48	zif_S_L23	vs.	PV_C_L4			0.919*	0.027		
zif268-GAD67 – across layers – across arcs									
49	zif_NS_L23	vs.	GAD67_C_L4	0.820*	0.046				
50	zif_S_L23	vs.	GAD67_C_L4	0.872*	0.024				
51	zif_C_L23	vs.	GAD67_C_L4			0.922*	0.026		
GAD67-PV – same layer – same arc									
52	GAD67_S_L4	vs.	PV_S_L4					-0.894*	0.041
GAD67-PV – same layer – across arcs									
53	GAD67_S_L4	vs.	PV_NS_L4					-0.930*	0.022
GAD67-PV – across layers – same arc									
54	GAD67_NS_L4	vs.	PV_NS_L23					-0.919*	0.027
GAD67-PV – across layers – across arcs									
55	GAD67_S_L4	vs.	PV_NS_L23	0.861*	0.028				
56	GAD67_C_L23	vs.	PV_S_L4			0.893*	0.041		

Matrices were established for the active-rTMS, sham-rTMS and control groups. Negative correlations are indicated in bold.

field. The principal N1 and P1 responses of LFPs declined by ~30% for the spared D2 and D3 barrel, although lateral spread of activity to adjacent barrels within the same row was affected differently. Responses in barrels caudal to the principal response were diminished even more than the principal response (~60%), whereas responses in

rostral barrels were not affected. Active rTMS restored the principal N1 amplitude to the control level and also increased responses spreading laterally to the caudal and rostral barrels. Although caudal responses increased to around the control level with iTBS, rostral responses were somewhat larger than those obtained from controls.

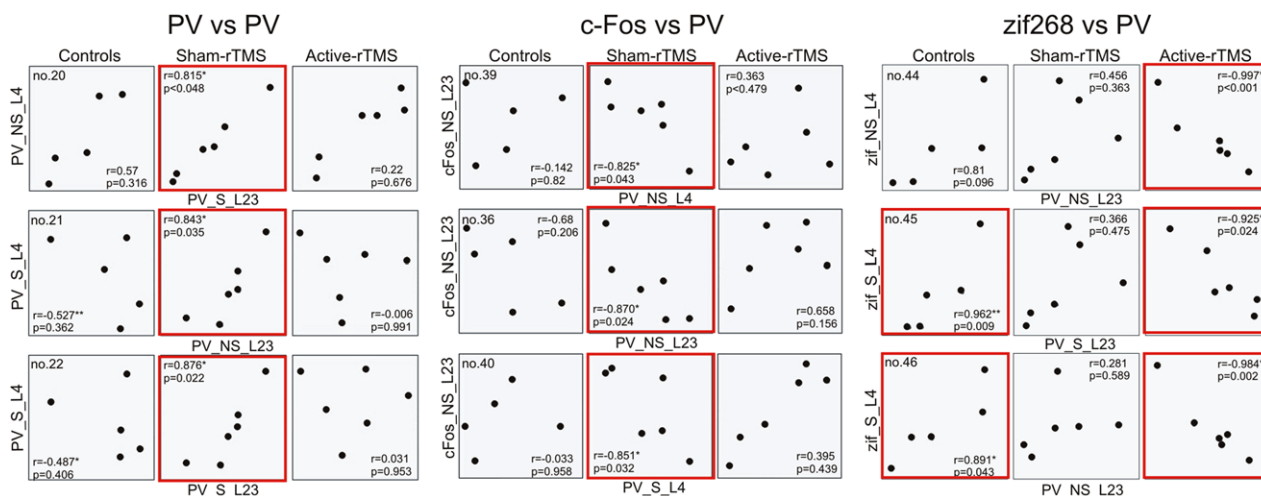
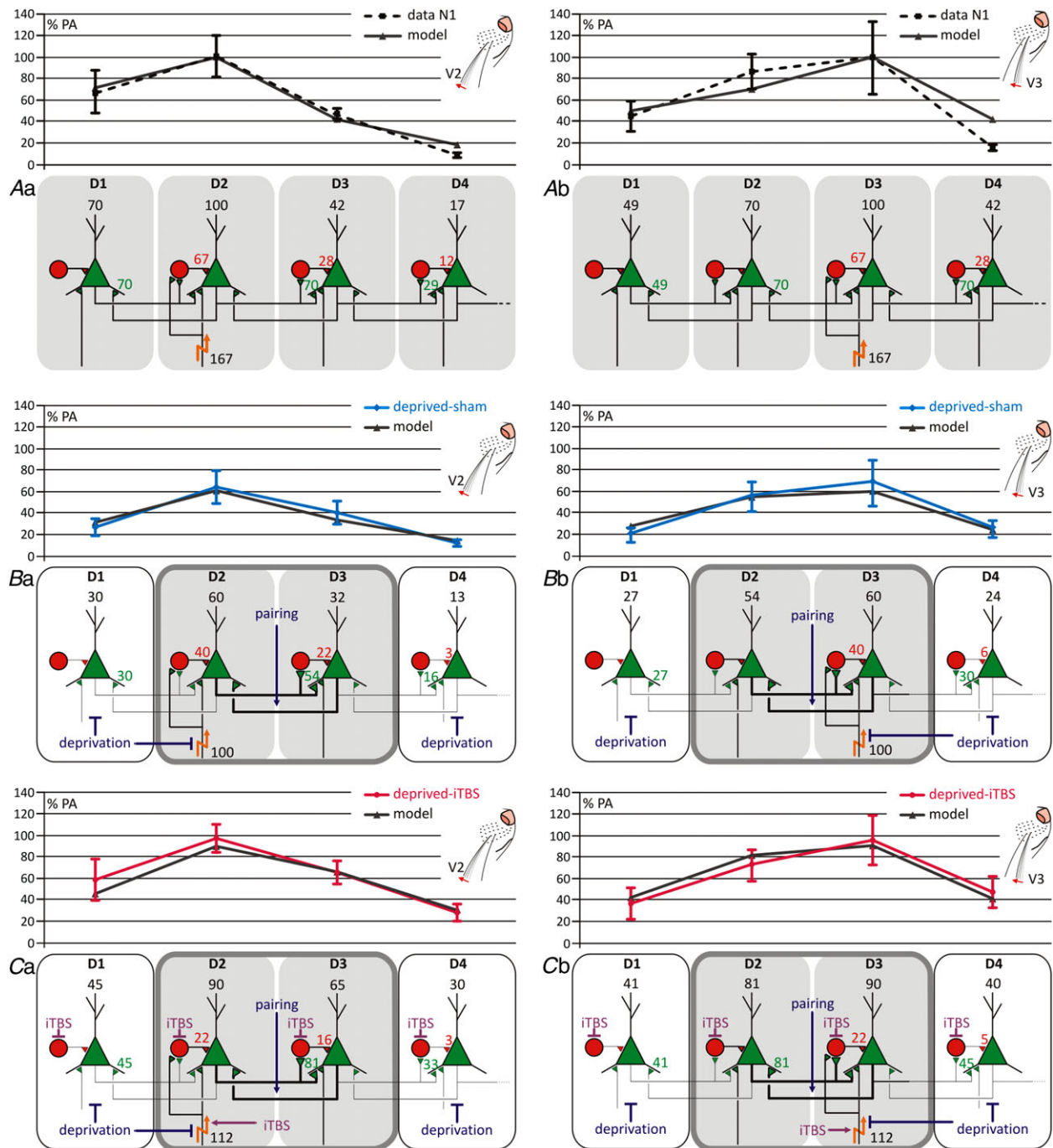


Figure 7. Correlations of cells labelled for different neuronal activity markers

Distribution of data points for significant cases (red frames) shown in Table 6 compared to the corresponding correlations of the other experimental groups. Left: cases 20–22; middle: cases 36, 39, 40; right: cases 44–46.

Former studies on the pairing of two whiskers in adult rats by removing all other whiskers of the pad revealed somewhat different, and in part controversial, results. Often, pairing was accompanied by more lateral spread of activity towards the barrel of the paired whisker and a

decline towards deafferented barrels (Diamond *et al.* 1993; Wallace & Sakmann 2008). On the other hand, Lebedev *et al.* (2000) reported that deafferented barrels show a stronger disinhibition than non-deafferented barrels and are more susceptible to plastic changes, thus following



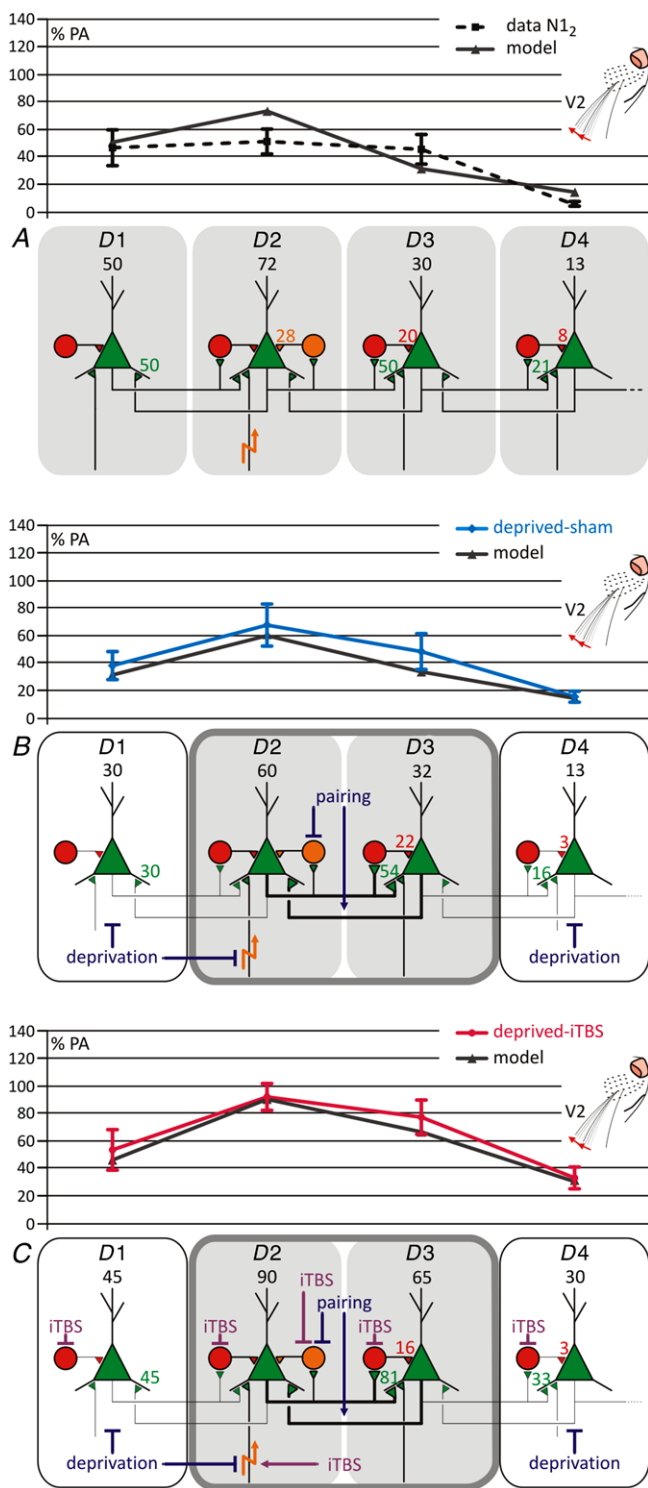


Figure 9. Same computational model for the case of double stimulation, including recurrent inhibition

Same model as shown in Fig. 8 but with recurrent inhibition (orange neurons) added to the otherwise unchanged lateral inhibition to calculate the changes in amplitude of the second response (N_{12}) to a pair of stimuli applied to whisker D2. A, control condition. B, deafferentation. C, deafferentation with iTBS. Additional explanation of the connection strengths and their variations is provided in the main text.

the rule of Bienenstock *et al.* (1982) according to an activity-dependent lowering of the dynamic threshold. Krieger (2009) found neurons in deafferented barrels (only one row) to show stronger dendritic calcium transients upon back-propagating action potentials and Schierloh *et al.* (2004) demonstrated increased projections from non-deafferented L4 to deafferented regions of L2/3, with both being signs of increased plasticity in deafferented columns. Our finding of generally lowered LFP responses after deafferentation may be related to two deviating conditions: (i) we did not spare two whiskers but two arcs and (ii) we forced rats to use their whiskers by exposing all of them to an enriched environment. The latter shows strong agreement with the findings of Polley *et al.* (1999), showing by optical imaging that whisker representations shrink rather than expand with whisker-guided exploration of a new environment. It is thus probable that disinhibition and increased lateral spread of cortical activity occurs as a result of reduced sensory activity.

As expected, LFP analysis further revealed that amplitudes of the early negative N1 and also that of the directly following positive P1 wave were generally larger with stimulation of the principal whisker compared to stimulation of a neighbouring whisker of the same row. In addition, we found an asymmetry, with larger response amplitudes in more caudal than rostral barrels not only with stimulation of the principal whisker, but also with lateral spread of activity. This finding is in accordance with earlier reports showing that stimulation of caudal and ventral whiskers induces a higher level of 2-deoxyglucose staining compared to rostral and dorsal whiskers (Durham & Woolsey, 1985; McCasland & Woolsey, 1988). This difference appears to be related to an asymmetric lateral cortical inhibition because paired stimulation with caudally and ventrally adjacent whiskers inhibits the principal whisker response much more than pairing with rostrally or dorsally located whiskers (Simons & Carvell, 1989). On the other hand, caudal barrels appear to project more strongly towards rostral barrels compared to the other way round (Lebedev *et al.* 2000). Generally, lateral spread of cortical activity within L2/3 is stronger along rows than arcs (Petersen *et al.* 2003). This type of asymmetry has not been found in the thalamic sensory relay (Brumberg *et al.* 1996) and appears to evolve as a result of horizontal cortical connections.

Electrophysiological studies were combined with immunohistochemical analyses to determine whether deafferentation and rTMS affected the basal or the stimulation-induced expression of neuronal activity markers. On the experimental side, we found that the number of c-Fos+ neurons was much higher in those barrels representing the selectively stimulated arc no. 2 compared to the contralateral barrel field being not manipulated, in particular in L4. This could be related

either to missing lateral inhibition from non-stimulated neighbouring arcs or to the effect of modulatory systems mediating attention effects to the single stimulated arc. The latter is in line with previous studies showing enhanced responsiveness of neurons in barrels related to spared whiskers (Diamond *et al.* 1993; Glazewski & Fox, 1996). The increase in responsiveness of spared barrels was previously found to be evident after 24 h (Diamond *et al.* 1994) and even after 15 h when animals were experiencing an enriched environment (Rema *et al.* 2006). Interestingly, the sham-rTMS group showed significantly lowered numbers of c-Fos+ (and to some degree zif268+) neurons in these barrels compared to the active-rTMS and control groups (at least in L4), which is in accordance with the lowered LFP amplitudes in this group because inducible immediate early genes are expressed in an activity-dependent manner (Herdegen & Leah, 1998). In addition, the numbers of GAD67+ (and in part PV+) neurons were higher throughout the experimental (deafferented) barrel field compared to controls, indicating that increased inhibition might be the reason for reduced LFP amplitudes. One reason for the increased activity of inhibitory neurons could be the influence of the non-deafferented and, consequently, more active contralateral barrel field. Enhanced transcallosal inhibition has been reported in stroke patients (Bertolucci *et al.* 2018) and stimulation of the axons of the corpus callosum evokes inhibition of layer 5 pyramidal cells of rat somatosensory cortex via upper layer interneurons (Murphy *et al.* 2016).

On the other hand, Akhtar and Land (1991) found decreased numbers of GAD+ terminals in deafferented barrel cortex, whereas selective artificial stimulation of a single whisker for 24 h increased the terminal density within the corresponding barrel with a dominance of GABAergic terminals (Knott *et al.* 2002). These findings appear to be partly in contrast to our results but, as discussed above, any differences may depend on the amount of whisker use during the deprivation episode and whether stimulation is passive or results from exploration (Polley *et al.* 1999).

It also appears that possible potentiation of spared and depression of deafferented barrels takes place simultaneously, depending on the degree and pattern of deafferentation (Diamond *et al.* 1993; Simons & Land, 1994; Shepherd *et al.* 2003; Wallace & Fox, 1999). The increase in LFP responses back to control level, and even above, in the active-rTMS group is not directly resembled by the distribution of GAD67+ and PV+ cells. However, rTMS (being non-focal within the small rat brain) affects not only the experimental side, but also the barrel field of the contralateral hemisphere. We found the expression of these inhibitory activity markers to be increased in the contralateral barrel field and therefore decided to apply an internal normalization between the

experimental and control barrel fields to unravel the differences between sham- and active-rTMS conditions specific to the experimental side. In this case, we found a significantly lower number of PV+ neurons within L2/3 of the active group compared to sham group, indicating that rTMS may have lowered inhibitory activity in these layers.

Our simple computational model was able to reproduce all of the experimental findings, the lowered response amplitudes with deafferentation and the recovery to control levels with active iTBS not only with regard to principal responses, but also with regard to the asymmetric lateral spread of activity to neighbouring barrels. This particular feature could be established by an asymmetric lateral inhibition (stronger in rostral direction) and by dampening this inhibition with iTBS. A further reduction in recurrent-type inhibition replicated the loss of inhibition of the second response in the double-stimulation paradigm. Deafferentation further led to a stronger excitatory coupling of the two spared arcs.

Our hypothesis that recurrent and lateral inhibition might be mediated by PV+ interneurons is supported by a recent study showing that optogenetic inhibition of PV+ neurons causes an increase in lateral excitation, whereas optogenetic activation causes a strong reduction (Yang *et al.* 2017). In addition, activation of PV+ interneurons is most efficient within a 20 ms window to reduce the responses of the principal barrel. Our model thus replicates the experimental data very well not only with regard to deafferentation and iTBS-rTMS effects, but also with regard to an asymmetry in lateral spread of activity. Other scenarios, such as the direct potentiation of excitatory synapses with iTBS, are also possible. However, *in vitro* data support the assumption that high-frequency rTMS more probably modulates inhibition, which subsequently enables potentiation of glutamatergic transmission (Vlachos *et al.* 2012; Lenz *et al.* 2016). The same TMS condition as that used by ourselves (i.e. inducing an electric field with mediolateral orientation using a figure-of-eight coil) was found to mainly target inhibitory interneurons within supragranular layers of rat somatosensory cortex (Murphy *et al.* 2016).

Sensory activity appears to regulate the expression of neurotrophins like brain-derived neurotrophic factor (BDNF) and nerve growth factor (Rossi *et al.* 1999; Gomez-Pinilla *et al.* 2011; Sun *et al.* 2014), which are able to modulate sensory activity in terms of strength and spatial distribution (Prakash *et al.* 1996). In particular, GABAergic circuits appear to be controlled by BDNF in an activity-dependent manner not only during early maturation (Hensch, 2005; Kaneko *et al.* 2012; Koh *et al.* 2016), but also in the adult state (Baroncelli *et al.* 2010; Jiao *et al.* 2011). The latter appears to be a key mechanism for controlling the degree of neuronal

plasticity in the adult state (Galuske *et al.* 1996; Maffei 2002; Risedal *et al.* 2002; Gianfranceschi *et al.* 2003). Environmental enrichment has been shown to trigger such processes (Sale *et al.* 2007). Recently, we could show that iTBS-rTMS applied to light-deprived (dark-reared) rats during an early critical period of use-dependent cortical development had almost the same beneficial effect on functional development visual cortex as that of an enriched environment (Castillo-Padilla & Funke, 2016) and was associated not only with modulation of cortical PV expression, but also with BDNF expression. The present study demonstrates that iTBS-rTMS can counteract the depression of sensory activity in deafferented areas of rat barrel cortex, a process probably related to a disinhibitory effect. Cortical regions with (transient) loss of sensory input or reduced activity as a result of a nearby lesion are often additionally inhibited by neighbouring cortical areas or transcallosal projections of the corresponding contralateral areas (Lissek *et al.* 2009; Ngomo *et al.* 2012; Bertolucci *et al.* 2018). Deprivation of sensory input not only for a few days, but also for weeks as a result of immobilization of limbs has been shown to reduce cortical excitability, which was evident as reduced motor-evoked potentials by TMS of the motor cortex (Facchini *et al.* 2002; Ngomo *et al.* 2012) and reduced sensory cortical activation as measured by functional resonance imaging, accompanied by impaired tactile acuity (Lissek *et al.* 2009). Thus, the experimental conditions that we investigated in rats appear to probably represent depressed states of human sensory or motor cortex evolving from an excitatory-inhibitory imbalance between normally active and impaired cortical regions. It remains to be tested whether the disinhibitory action achieved with iTBS-rTMS (Funke & Benali, 2011; Hamada *et al.* 2013; Suppa *et al.* 2016) has better therapeutic effects on speeding up functional recovery when applied during the acute phase of disturbance compared to later applications.

Study limitations

One limitation of the present study in translational terms is the non-focality of the applied rTMS, which was unable to specifically target the barrel cortex directly, and hence probably modulated the activity of this cortical area only via its callosal inputs. Accordingly, activity was primarily induced in the superficial cortical layers not only transsynaptically, but also via retrograde activation of layer 2/3 pyramidal cells and their axon collaterals, although this obviously was not sufficiently strong to activate the deep projection cells of layer 5, as similarly demonstrated by Murphy *et al.* (2016). Moreover, as reported by Rotenberg *et al.* (2010), a stimulation intensity of more than 80% machine output is required to activate

spinally projecting pyramidal cells directly. The low level of stimulation intensity (23% machine output) applied to activate the callosal axons in rats is advantageous because the probability of stimulating brain areas other than those intended is rather low. Thus, this stimulation condition appears to be similar to stimulation of the human neocortex at intensities below the threshold that evokes motor potentials, which is considered to be related to the activation of horizontally travelling axons within the upper cortical layers. However, by contrast to human rTMS conditions, we stimulated multiple cortical areas of both hemispheres in this way.

References

- Abraham WC, Mason SE, Demmer J, Williams JM, Richardson CL, Tate WP, Law PA, Dragunow M (1993). Correlations between immediate early gene induction and the persistence of long-term potentiation. *Neurosci* **56**, 717–727.
- Akhtar ND & Land PW (1991). Activity-dependent regulation of glutamic acid decarboxylase in the rat barrel cortex: effects of neonatal versus adult sensory deprivation. *J Comp Neurol* **307**, 200–213.
- Allen CB, Celikel T & Feldman DE (2003). Long-term depression induced by sensory deprivation during cortical map plasticity in vivo. *Nat Neurosci* **6**, 291–299.
- Amrhein V, Greenland S, McShane B (2019). Scientists rise up against statistical significance. *Nature* **567**, 305–307.
- Baroncelli L, Sale A, Viegi A, Maya Vetencourt JF, De Pasquale R, Baldini S & Maffei L (2010). Experience-dependent reactivation of ocular dominance plasticity in the adult visual cortex. *Exp Neurol* **226**, 100–109.
- Benali A, Trippe J, Weiler E, Mix A, Petrasch-Parwez E, Girzalsky W, Eysel UT, Erdmann R & Funke K (2011). Theta-burst transcranial magnetic stimulation alters cortical inhibition. *J Neurosci* **31**, 1193–1203.
- Benes FM & Berretta S (2001). GABAergic interneurons: implications for understanding schizophrenia and bipolar disorder. *Neuropsychopharmacology* **25**, 1–27.
- Bertolucci F, Chisari C, Fregni F (2018). The potential dual role of transcallosal inhibition in post-stroke motor recovery. *Restor Neurol Neurosci* **36**, 83–97.
- Bienenstock EL, Cooper LN & Munro PW (1982). Theory for the development of neuron selectivity: orientation specificity and binocular interaction in visual cortex. *J Neurosci* **2**, 32–48.
- Brumberg JC, Pinto DJ & Simons DJ (1996). Spatial gradients and inhibitory summation in the rat whisker barrel system. *J Neurophysiol* **76**, 130–140.
- Caillard O, Moreno H, Schwaller B, Llano I, Celio MR, Marty A (2000). Role of the calcium-binding protein parvalbumin in short-term synaptic plasticity. *PNAS* **97**, 13372–13377.
- Cardin JA (2018). Inhibitory interneurons regulate temporal precision and correlations in cortical circuits. *Trends Neurosci* **41**, 689–700.
- Caroni P (2015). Regulation of parvalbumin basket cell plasticity in rule learning. *Biochem Biophys Res Commun* **460**, 100–103.

- Castillo-Padilla DV & Funke K (2016). Effects of chronic iTBS-rTMS and enriched environment on visual cortex early critical period and visual pattern discrimination in dark-reared rats. *Dev Neurobiol* **76**, 19–33.
- Dayan E, Censor N, Buch ER, Sandrini M & Cohen LG (2013). Noninvasive brain stimulation: from physiology to network dynamics and back. *Nat Neurosci* **16**, 838–844.
- Diamond ME, Armstrong-James M & Ebner FF (1993). Experience-dependent plasticity in adult rat barrel cortex. *Proc Natl Acad Sci U S A* **90**, 2082–2086.
- Diamond ME, Huang W & Ebner FF (1994). Laminar comparison of somatosensory cortical plasticity. *Science* **265**, 1885–1888.
- Di Pino G, Pellegrino G, Assenza G, Capone F, Ferreri F, Formica D, Ranieri F, Tombini M, Ziemann U, Rothwell JC & Di Lazzaro V (2014). Modulation of brain plasticity in stroke: a novel model for neurorehabilitation. *Nat Rev Neurol* **10**, 597–608.
- Durham D & Woolsey TA (1985). Functional organization in cortical barrels of normal and vibrissae-damaged mice: a (3H) 2-deoxyglucose study. *J Comp Neurol* **235**, 97–110.
- Facchini S, Romani M, Tinazzi M, Aglioti SM (2002). Time-related changes of excitability of the human motor system contingent upon immobilisation of the ring and little fingers. *Clin Neurophysiol* **113**, 367–375.
- Feldman DE & Brecht M (2005). Map plasticity in somatosensory cortex. *Science* **310**, 810–815.
- Finnerty G.T, Roberts LS & Connors BW (1999). Sensory experience modifies the short-term dynamics of neocortical synapses. *Nature* **400**, 367–371.
- Fox K (1992). A critical period for experience-dependent synaptic plasticity in rat barrel cortex. *J Neurosci* **12**, 1826–1838.
- Fox K (2002). Anatomical pathways and molecular mechanisms for plasticity in the barrel cortex. *Neurosci* **111**, 799–814.
- Fox K (2008). *Barrel Cortex*. Cambridge University Press. <https://doi.org/10.1017/CBO9780511541636>.
- Froemke RC (2015). Plasticity of cortical excitatory-inhibitory balance. *Annu Rev Neurosci* **38**, 195–219.
- Funke K & Benali A (2011). Modulation of cortical inhibition by rTMS – findings obtained from animal models. *J Physiol* **589**, 4423–4435.
- Galuske RA, Kim DS, Castren E, Thoenen H & Singer W (1996). Brain-derived neurotrophic factor reversed experience-dependent synaptic modifications in kitten visual cortex. *Eur J Neurosci* **8**, 1554–1559.
- Gianfranceschi L, Siciliano R, Walls J, Morales B, Kirkwood A, Huang ZJ, Tonegawa S & Maffei L (2003). Visual cortex is rescued from the effects of dark rearing by overexpression of BDNF. *Proc Natl Acad Sci U S A* **100**, 12486–12491.
- Glazewski S & Fox K (1996). Time course of experience-dependent synaptic potentiation and depression in barrel cortex of adolescent rats. *J Neurophysiol* **75**, 1714–1729.
- Gomez-Pinilla F, Ying Z, Agoncillo T & Frostig R (2011). The influence of naturalistic experience on plasticity markers in somatosensory cortex and hippocampus: effects of whisker use. *Brain Res* **1388**, 39–47.
- Gonzalez-Burgos G, Cho RY & Lewis DA (2015). Alterations in cortical network oscillations and parvalbumin neurons in schizophrenia. *Biol Psychiatry* **77**, 1031–40.
- Grundy D (2015). Principles and standards for reporting animal experiments in The Journal of Physiology and Experimental Physiology. *Exp Physiol* **100**, 755–758.
- Hamada M, Murase N, Hasan A, Balaratnam M & Rothwell JC (2013). The role of interneuron networks in driving human motor cortical plasticity. *Cereb Cortex* **23**, 1593–1605.
- Hensch TK (2005). Critical period plasticity in local cortical circuits. *Nat Rev Neurosci* **6**, 877–888.
- Herdegen T & Leah JD (1998). Inducible and constitutive transcription factors in the mammalian nervous system: control of gene expression by Jun, Fos and Krox and REB/ATF proteins. *Brain Res Rev* **28**, 370–490.
- Hoppenrath K & Funke K (2013). Time-course of changes in neuronal activity markers following iTBS-TMS of the rat neocortex. *Neurosci Lett* **536**, 19–23.
- Huang YZ, Edwards MJ, Rounis E, Bhatia KP & Rothwell JC (2005). Theta burst stimulation of the human motor cortex. *Neuron* **45**, 201–206.
- Huang YZ, Sommer M, Thickbroom G, Hamada M, Pascual-Leonne A, Paulus W, Classen J, Peterchev AV, Zangen A & Ugawa Y (2009). Consensus: new methodologies for brain stimulation. *Brain Stimul* **2**, 2–13.
- House DR, Elstrott J, Koh E, Chung J & Feldman DE (2011). Parallel regulation of feedforward inhibition and excitation during whisker map plasticity. *Neuron* **72**, 819–831.
- Hubel DH & Wiesel TN (1964). Effects of monocular deprivation in kittens. *Naunyn Schmiedebergs Arch Exp Pathol Pharmacol* **248**, 492–497.
- Jazmati D, Neubacher U, Funke K (2018). Neuropeptide Y as a possible homeostatic element for changes in cortical excitability induced by repetitive transcranial magnetic stimulation. *Brain Stimul* **11**, 797–805.
- Jiao Y, Zhang Z, Zhang C, Wang X, Sakata K, Lu B & Sun QQ (2011). A key mechanism underlying sensory experience-dependent maturation of neocortical GABAergic circuits in vivo. *Proc Natl Acad Sci U S A* **108**, 12131–12136.
- Kaneko M, Xie Y, An JJ, Stryker MP & Xu B (2012). Dendritic BDNF synthesis is required for late-phase spine maturation and recovery of cortical responses following sensory deprivation. *J Neurosci* **32**, 4790–4802.
- Kawaguchi Y & Kubota Y (1998). Neurochemical features and synaptic connections of large physiologically-identified GABAergic cells in the rat frontal cortex. *Neuroscience* **85**, 677–701.
- Knott GW, Quairiaux C, Genoud C & Welker E (2002). Formation of dendritic spines with GABAergic synapses induced by whisker stimulation in adult mice. *Neuron* **34**, 265–273.
- Koh DX & Sng JC (2016). HDAC1 negatively regulates Bdnf and Pvalb required for parvalbumin interneuron maturation in an experience-dependent manner. *J Neurochem* **139**, 369–380.
- Kossut M & Hand P (1984). Early development of changes in cortical representation of C3 vibrissa following neonatal denervation of surrounding vibrissa receptors: a 2-deoxyglucose study in the rat. *Neurosci Lett* **46**, 7–12.

- Krieger P (2009). Experience-dependent increase in spine calcium evoked by backpropagating action potentials in layer 2/3 pyramidal neurons in rat somatosensory cortex. *Eur J Neurosci* **30**, 1870–1877.
- Lebedev MA, Mirabella G, Erchova I & Diamond ME (2000). Experience-dependent plasticity of rat barrel cortex: redistribution of activity across barrel-columns. *Cereb Cortex* **10**, 23–31.
- Lenz M, Galanis C, Müller-Dahlhaus F, Opitz A, Wierenga CJ, Szabó G, Ziemann U, Deller T, Funke K & Vlachos A (2016). Repetitive magnetic stimulation induces plasticity of inhibitory synapses. *Nat Comm* **7**, 10020.
- Letzkus JJ, Wolff SB & Lüthi A (2015). Disinhibition, a circuit mechanism for associative learning and memory. *Neuron* **88**, 264–276.
- Lewis DA (2014). Inhibitory neurons in human cortical circuits: substrate for cognitive dysfunction in schizophrenia. *Curr Opin Neurobiol* **26**, 22–26.
- Lissek S, Wilimzig C, Stude P, Pleger B, Kalisch T, Maier C, Peters SA, Nicolas V, Tegenthoff M, Dinse HR (2009). Immobilization impairs tactile perception and shrinks somatosensory cortical maps. *Curr Biol*; **19**, 837–842.
- Maffei L (2002). Plasticity in the visual system: role of neurotrophins and electrical activity. *Arch Ital Biol* **140**, 341–346.
- Margolis DJ, Lütcke H & Helmchen F (2014). Microcircuit dynamics of map plasticity in barrel cortex. *Curr Opin Neurobiol* **24**, 76–81.
- Markram H, Toledo-Rodriguez M, Wang Y, Gupta A, Silberberg G & Wu C (2004). Interneurons of the neocortical inhibitory system. *Nat Rev Neurosci* **5**, 793–807.
- McCasland JS & Woolsey TA (1988). High-resolution 2-deoxyglucose mapping of functional cortical columns in mouse barrel cortex. *J Comp Neurol* **278**, 555–569.
- Merzenich MM, Kaas JH, Wall J, Nelson RJ, Sur M & Felleman D (1983). Topographic reorganization of somatosensory cortical areas 3b and 1 in adult monkeys following restricted deafferentation. *Neuroscience* **8**, 33–55.
- Mix A, Benali A, Eysel UT & Funke K (2010). Continuous and intermittent transcranial magnetic theta burst stimulation modify tactile learning performance and cortical protein expression in the rat differently. *Eur J Neurosci* **32**, 1575–1586.
- Murphy SC, Palmer LM, Nyffeler T, Müri RM & Larkum ME (2016). Transcranial magnetic stimulation (TMS) inhibits cortical dendrites. *Elife* **5**, e13598.
- Ngomo S, Leonard G, Mercier C (2012). Influence of the amount of use on hand motor cortex representation: effects of immobilization and motor training. *Neuroscience* **220**, 208–214.
- Orduz D, Bishop DP, Schwaller B, Schiffmann SN, Gall D (2013). Parvalbumin tunes spike-timing and efferent short-term plasticity in striatal fast spiking interneurons. *J Physiol* **591**, 3215–3232.
- Petersen CC (2007). The functional organization of the barrel cortex. *Neuron* **56**, 339–355.
- Petersen CC, Grinvald A & Sakmann B (2003). Spatiotemporal dynamics of sensory responses in layer 2/3 of rat barrel cortex measured in vivo by voltage-sensitive dye imaging combined with whole-cell voltage recordings and neuron reconstructions. *J Neurosci* **23**, 1298–1309.
- Polley DB, Chen-Bee CH & Frostig RD (1999). Varying the degree of single-whisker stimulation differentially affects phases of intrinsic signals in rat barrel cortex. *J Neurophysiol* **81**, 692–701.
- Prakash N, Cohen-Cory S & Frostig RD (1996). Rapid and opposite effects of BDNF and NGF on the functional organization of the adult cortex in vivo. *Nature* **381**, 702–706.
- Ragert P, Franzkowiak S, Schwenkreis P, Tegenthoff M, Dinse HR (2008). Improvement of tactile perception and enhancement of cortical excitability through intermittent theta burst rTMS over human primary somatosensory cortex. *Exp Brain Res* **184**, 1–11.
- Rema V, Armstrong-James M, Jenkinson N & Ebner FF (2006). Short exposure to an enriched environment accelerates plasticity in the barrel cortex of adult rats. *Neuroscience* **140**, 659–672.
- Ridding MC & Ziemann U (2010). Determinants of the induction of cortical plasticity by non-invasive brain stimulation in healthy subjects. *J Physiol* **588**, 2291–2304.
- Risedal A, Mattsson B, Dahlqvist P, Nordborg C, Olsson T & Johansson BB (2002). Environmental influences on functional outcome after a cortical infarct in the rat. *Brain Res Bull* **58**, 315–321.
- Rossi FM, Bozzi Y, Pizzorusso T & Maffei L (1999). Monocular deprivation decreases brain-derived neurotrophic factor immunoreactivity in the rat visual cortex. *Neuroscience* **90**, 363–368.
- Rotenberg A, Muller PA, Vahabzadeh-Hagh AM, Navarro X, López-Vales R, Pascual-Leone A & Jensen F (2010). Lateralization of forelimb motor evoked potentials by transcranial magnetic stimulation in rats. *Clin Neurophysiol* **121**, 104–108.
- Sale A, Maya Vetencourt JF, Medini P, Cenni MC, Baroncelli L, De Pasquale R & Maffei L (2007). Environmental enrichment in adulthood promotes amblyopia recovery through a reduction of intracortical inhibition. *Nat Neurosci* **10**, 679–81.
- Schierloh A, Eder M, Zieglgänsberger W & Dodt HU (2004). Effects of sensory deprivation on columnar organization of neuronal circuits in the rat barrel cortex. *Eur J Neurosci* **20**, 1118–1124.
- Schmidt-Wilcke T, Fuchs E, Funke K, Vlachos A, Müller-Dahlhaus F, Puts NAJ, Harris RE & Edden RAE (2018). GABA—from inhibition to cognition: emerging concepts. *Neuroscientist* **24**, 501–515.
- Shepherd GMG, Pologruto TA & Svoboda K (2003). Circuit analysis of experience-dependent plasticity in the developing rat barrel cortex. *Neuron* **38**, 277–289.
- Simons DJ & Carvell GE (1989). Thalamocortical response transformation in the rat vibrissa/barrel system. *J Neurophysiol* **61**, 311–330.
- Simons DJ & Land PW (1994). Neonatal whisker trimming produces greater effects in nondeprived than deprived thalamic barreloids. *J Neurophysiol* **72**, 1434–1437.
- Sun QQ, Zhang Z, Sun J, Nair AS, Petrus DP & Zhang C (2014). Functional and structural specific roles of activity-driven BDNF within circuits formed by single spiny stellate neurons of the barrel cortex. *Front Cell Neurosci* **8**, 372.

- Suppa A, Huang YZ, Funke K, Ridding MC, Cheeran B, Di Lazzaro V, Ziemann U & Rothwell JC (2016). Ten years of theta burst stimulation in humans: established knowledge, unknowns and prospects. *Brain Stimul* **9**, 323–335.
- Tang AD, Lowe AS, Garrett AR, Woodward R, Bennett W, Canty AJ, Garry MI, Hinder MR, Summers JJ, Gersner R, Rotenberg A, Thickbroom G, Walton J, Rodger J (2016). Construction and evaluation of rodent-specific rTMS coils. *Front Neural Circuits* **10**, 47.
- Tegenthoff M, Ragert P, Pleger B, Schwenkreis P, Förster AF, Nicolas V, Dinse HR (2003). Improvement of tactile discrimination performance and enlargement of cortical somatosensory maps after 5 Hz rTMS. *PLoS Biol* **3**, e362.
- Thickbroom GW (2007). Transcranial magnetic stimulation and synaptic plasticity: experimental framework and human models. *Exp Brain Res* **180**, 583–593.
- Thimm A & Funke K (2015). Multiple blocks of intermittent and continuous theta-burst stimulation applied via transcranial magnetic stimulation differently affect sensory responses in rat barrel cortex. *J Physiol* **593**, 967–985.
- Trippe J, Mix A, Aydin-Abidin S, Funke K & Benali A (2009). Theta burst and conventional low frequency rTMS differentially affect GABAergic neurotransmission in the rat cortex. *Exp Brain Res* **199**, 411–421.
- Vlachos A, Müller-Dahlhaus F, Roskopp J, Lenz M, Ziemann U & Deller T (2012). Repetitive magnetic stimulation induces functional and structural plasticity of excitatory postsynapses in mouse organotypic hippocampal slice cultures. *J Neurosci* **32**, 17514–17523.
- Volk DW & Lewis DA (2014). Early developmental disturbances of cortical inhibitory neurons: contribution to cognitive deficits in schizophrenia. *Schizophr Bull* **40**, 952–957.
- Volz LJ, Benali A, Mix A, Neubacher U & Funke K (2013). Dose-dependence of changes in cortical protein expression induced with repeated transcranial magnetic theta-burst stimulation in the rat. *Brain Stimul* **6**, 598–606.
- Vreugdenhil M, Jefferys JGR, Celio MR, Schwaller B (2003). Parvalbumin-deficiency facilitates repetitive IPSCs and gamma oscillations in the hippocampus. *J Neurophysiol* **89**, 1414–1422.
- Wallace DJ & Sakmann B (2008). Plasticity of representational maps in somatosensory cortex observed by in vivo voltage-sensitive dye imaging. *Cereb Cortex* **18**, 1361–1373.
- Wallace H & Fox K (1999). The effect of vibrissa deprivation pattern on the form of plasticity induced in rat barrel cortex. *Somatosens Mot Res* **16**, 122–138.
- Wong-Riley M (1979). Changes in the visual system of monocularly sutured or enucleated cats demonstrable with cytochrome oxidase histochemistry. *Brain Res* **171**, 11–28.
- Yang JW, Prouvot PH, Reyes-Puerta V, Stüttgen MC, Stroh A & Luhmann HJ (2017). Optogenetic modulation of a minor fraction of parvalbumin-positive interneurons specifically affects spatiotemporal dynamics of spontaneous and sensory-evoked activity in mouse somatosensory cortex in vivo. *Cereb Cortex* **27**, 5784–5803.
- Ziemann U & Siebner HR (2008). Modifying motor learning through gating and homeostatic metaplasticity. *Brain Stimul* **1**, 60–66.

Additional information

Competing interests

The authors declare that they have no competing interests.

Author contributions

EK conducted the experiments and analysed the electrophysiological and data immunohistological as part of her PhD thesis. The experiments were carried out in the Department of Neurophysiology, Ruhr-University Bochum. KF designed the study as part of the SFB874 project A4, proofed the data analysis and statistics and wrote the manuscript.

Funding

Funded by the Deutsche Forschungsgemeinschaft (DFG, German Research Foundation) – Projektnummer 122679504 – SFB 874.

Acknowledgements

The authors gratefully acknowledge the help of Ute Neubacher, Dimitrula Winkler, Christina Liebig and Tanja Ishorst for support with immunohistochemical techniques and animal handling. Thanks are also extended to Alia Benali and Patrik Krieger for proofreading the manuscript submitted for publication.